Xenopus Kazrin interacts with ARVCF-catenin, spectrin and p190B RhoGAP, and modulates RhoA activity and epithelial integrity

Kyucheol Cho[1,2,*], Travis G. Vaught[1,2,*], Hong Ji[1], Dongmin Gu[1,2], Catherine Papasakelariou-Yared[1,2], Nicola Horstmann[1], Jean Marie Jennings[3], Moonsup Lee[1,2], Lisa M. Sevilla[4], Malgorzata Kloc[5], Albert B. Reynolds[6], Fiona M. Watt[4], Richard G. Brennan[1,2], Andrew P. Kowalczyk[3] and Pierre D. McCrea[1,2,‡]

[1]Department of Biochemistry and Molecular Biology, The University of Texas M. D. Anderson Cancer Center, 1515 Holcombe Boulevard, Houston, TX 77030, USA
[2]Program in Genes and Development, University of Texas Graduate School of Biomedical Science, Houston, TX 77030, USA
[3]Department of Dermatology and Cell Biology, Emory University school of Medicine, Atlanta, GA 30322, USA
[4]Epithelial Cell Biology Laboratory, Cancer Research UK Cambridge Research Institute, Li Ka Shing Centre, Robinson Way, Cambridge CB2 0RE, UK
[5]Immuno-biology Laboratory, The Methodist Hospital Research Institute, The Methodist Hospital 6565 Fannin Street, Houston, TX 77030, USA
[6]Vanderbilt University Medical Center, 440-C Preston Building, Nashville, TN 37232-6840, USA

*These authors contributed equally to this work
‡Author for correspondence (pdmccrea@mdanderson.org)

Accepted 16 August 2010
Journal of Cell Science 123, 4128-4144

doi:10.1242/jcs.072041

Summary

In common with other p120-catenin subfamily members, *Xenopus* ARVCF (xARVCF) binds cadherin cytoplasmic domains to enhance cadherin metabolic stability or, when dissociated, modulates Rho-family GTPases. We report here that xARVCF binds and is stabilized by *Xenopus* KazrinA (xKazrinA), a widely expressed conserved protein that bears little homology to established protein families, and which is known to influence keratinocyte proliferation and differentiation and cytoskeletal activity. Although we found that xKazrinA binds directly to xARVCF, we did not resolve xKazrinA within a larger ternary complex with cadherin, nor did it co-precipitate with core desmosomal components. Instead, screening revealed that xKazrinA binds spectrin, suggesting a potential means by which xKazrinA localizes to cell–cell borders. This was supported by the resolution of a ternary biochemical complex of xARVCF–xKazrinA–xβ2-spectrin and, in vivo, by the finding that ectodermal shedding followed depletion of xKazrin in *Xenopus* embryos, a phenotype partially rescued with exogenous xARVCF. Cell shedding appeared to be the consequence of RhoA activation, and thereby altered actin organization and cadherin function. Indeed, we also revealed that xKazrinA binds p190B RhoGAP, which was likewise capable of rescuing Kazrin depletion. Finally, xKazrinA was found to associate with δ-catenins and p0071-catenins but not with p120-catenin, suggesting that Kazrin interacts selectively with additional members of the p120-catenin subfamily. Taken together, our study supports the essential role of Kazrin in development, and reveals the biochemical and functional association of KazrinA with ARVCF-catenin, spectrin and p190B RhoGAP.

Key words: ARVCF, Cadherin, Kazrin

Introduction

Catenins were initially defined as molecules that bind cadherins (Ozawa et al., 1989) and, with the exception of α-catenin, that possess a central Armadillo (Arm) domain that mediates cadherin and other protein–protein interactions (Choi and Weis, 2005; Huber et al., 1997; Peifer et al., 1994). Catenins have numerous roles in varied cellular compartments. Members of the p120-catenin subfamily, such as p120-catenin, Armadillo-repeat protein deleted in velo-cardio-facial syndrome (ARVCF)-catenin and δ-catenin, modulate cadherin stability at cell–cell junctions (Davis et al., 2003; Fang et al., 2004; Gu et al., 2009; Ireton et al., 2002; Xiao et al., 2003). They also directly or indirectly associate with and regulate small GTPases, enabling intracellular signaling and cytoskeletal control (for a review, see Anastasiadis, 2007). Most catenins additionally enter the nucleus (for a review, see McCrea et al., 2009). β-catenin, for example, is known to relieve TCF/LEF-mediated transcriptional repression in response to canonical Wnt-pathway stimulation, thereby activating target genes important in development or in pathologies such as cancer (for a review, see Cadigan and Peifer, 2009). Although further study is required to address unresolved issues (Ruzov et al., 2009a; Ruzov et al., 2009b), we and others find that p120 likewise contributes to Wnt signaling (Hong et al., 2010; Iioka et al., 2009; Kim et al., 2004; Park et al., 2006; Park et al., 2005; Spring et al., 2005). In comparison to β-catenin and p120-catenin, relatively little is known concerning the interactions and functional roles of ARVCF-catenin or other catenins.

ARVCF is one of several gene products deleted in velo-cardio facial syndrome (Sirotkin et al., 1997). In the context of the cadherin complex, p120 subfamily members including ARVCF bind in a mutually exclusive manner to the cadherin juxtamembrane domain (Mariner et al., 2000). In the nucleus, p120- but not ARVCF-catenin binds the transcriptional repressor Kaiso (Daniel and Reynolds, 1999; Kim et al., 2002) (for a review, see Daniel, 2007). The C-terminal PDZ binding motifs within ARVCF, δ-catenin and p0071 (absent in p120-catenin) bind the ERBIN scaffolding protein (Laura et al., 2002), the ZO-1 and ZO-2 tight junction proteins (Kausalya et al., 2004), and the less-characterized

FRMPD2 (Stenzel et al., 2009). In brief, the p120-subclass proteins exhibit both shared and non-overlapping interactions.

To reveal novel ARVCF functions, we screened a *Xenopus* neurula (stage 18) cDNA library for proteins that interact with *Xenopus laevis* ARVCF (xARVCF) and identified *Xenopus laevis* Kazrin (xKazrinA). Biochemically, human KazrinA was previously shown to associate with the peripheral desmosomal proteins periplakin and envoplakin in human keratinocytes (Groot et al., 2004), with microtubules (isoformE) (Nachat et al., 2009), and to modulate RhoA (Sevilla et al., 2008a). We found that xKazrinA interacts directly with xARVCF but not with *Xenopus laevis* p120 (Xp120) or β-catenin, and as reported earlier is present at cell–cell junctions (Groot et al., 2004). Surprisingly, we found that the xARVCF–xKazrinA complex associates and colocalizes with the spectrin cytoskeleton, rather than with cadherins at adherens junctions (Kaufmann et al., 2000; Mariner et al., 2000; Paulson et al., 2000), or with desmosomal core proteins (Groot et al., 2004). Our depletion of xKazrinA resulted in lessened embryonic tissue integrity (Sevilla et al., 2008b). In parallel, xARVCF protein levels were reduced and, supporting their functional interaction, exogenous xARVCF significantly rescued xKazrinA depletion phenotypes. xKazrinA depletion additionally led to RhoA activation, microfilament alterations, and lowered cadherin and cell adhesion levels, which are probably relevant to ectodermal fragility. An additional screen for novel xKazrinA partners resolved Xp190B RhoGAP. In common with xARVCF, p190B partially rescued xKazrinA depletion effects, consistent with functional links existing between components of the xARVCF–xKazrinA–Xp190B complex. Finally, two additional *Xenopus* p120 subfamily catenins, xδ-catenin and Xp0071 directly bound xKazrinA. Taken together, we propose that xKazrinA enables xARVCF association with the spectrin–actin network, and that the xARVCF–xKazrinA–Xp190B complex modulates RhoA activity and thereby cytoskeletal organization, cell adhesion and ectodermal integrity.

Results

Yeast two-hybrid analysis identifies a novel ARVCF-associated protein

Yeast two-hybrid analysis, using xARVCF as 'bait', was employed to screen a *X. laevis* stage18 neurula library for interacting proteins. Three independent clones corresponded to the *X. laevis* homolog of human KIAA1026 (GenBank accession #AB028949) (Kikuno et al., 1999). The fidelity of the screen was indicated by retrieving cadherin juxtamembrane domains known to bind p120-subclass catenins (data not shown) (Aono et al., 1999; Kaufmann et al., 2000; Mariner et al., 2000; Ohkubo and Ozawa, 1999; Ozawa and Kemler, 1998; Paulson et al., 2000; Thoreson et al., 2000; Yap et al., 1998). KIAA1026 became termed Kazrin (Groot et al., 2004). BLAST analysis demonstrated that xKazrin is highly homologous to human and mouse KazrinA (81% and 80.5% amino acid identity, respectively) (Table 1), and with *X. tropicalis* Kazrin (GenBank #EU404187; 92.6% identity) (Table 1) (Fig. 1A). Relative to xKazrin, *X. tropicalis* Kazrin contained 28 additional residues following the putative coiled-coil domain of Kazrin. RT-PCR and subsequent DNA sequencing of *X. laevis* stage18 neurula cDNA showed that this region (encoding the same 28 residues/exon 6) is alternatively spliced (Fig. 1B,D; data not shown). In keeping with another report (Groot et al., 2004), we named the short xKazrin isoform xKazrinA (structurally similar to human KazrinA), and the longer isoform xKazrinB.

Prior findings demonstrated that seven human Kazrin splice isoforms (KazrinA–KazrinF and KIAA1026) contain variable N- and C-termini (Groot et al., 2004; Kikuno et al., 1999; Nachat et al., 2009; Wang et al., 2009). As discussed below, KazrinA–KazrinF each encode a putative nuclear localization sequence (NLS), as do the *Xenopus* isoforms when assessed using PredictNLS server (http://cubic.bioc.columbia.edu.predictNLS) (Cokol et al., 2000) (Fig. 1A,C). KIAA1026, on the other hand, lacks this cluster of multiple lysine residues; we have designated KIAA1026 as KazrinK. As a preliminary test of the putative NLS functionality, we compared xKazrinA intracellular localization with that of human KazrinK (KIAA1026) in MCF7 cells. Human KazrinK appeared fully excluded, although xKazrinA resided in the nuclei of multiple cells (supplementary material Fig. S1A). This pattern was likewise observed in HEK293 and *Xenopus* A6 cells (data not shown). The putative NLS lysine residues of xKazrin (365–368; supplementary material Fig. S1B), were then mutated to glutamines to alter their charge but maintain the steric properties of the region (Cokol et al., 2000). Whereas full-length xKazrinA exhibited an even pattern within the cytoplasm and nucleus, or showed predominantly nuclear staining (supplementary material Fig. S1C, left panel), the NLS mutant was excluded from the nucleus. Collectively, these data suggest that the C-terminal polylysine tract of xKazrin functions as an NLS. Although KazrinK and KazrinE isoforms are represented in other mammals, we have not yet identified their homologs in *Xenopus*. In all cases, the existence of variably spliced and localized Kazrin isoforms is suggestive of functional distinctions.

Using predictive software, the central region of xKazrin and a limited N-terminal region (amino acids 82–255 and 16–41, respectively) were strongly predicted to be coiled coils (both scoring >90% using COILS) (http://www.ch.embnet.org/software/COILS_form.html) (Lupas et al., 1991). This region bears limited sequence similarity with known coiled-coil domains (Table 2). Using the structural property of 3.5 amino acid residues per helical turn, we modeled five coiled coils within the central region of xKazrin (leucine zipper), and an additional coil in the N-terminal region (supplementary material Fig. S1B and Fig. S2).

Table 1. Amino-acid comparison of xKazrinA with KazrinA proteins from human, mouse, rat, *X. tropicalis* and puffer fish (*Tetraodon nigroviridis*)

Organism	GenBank protein ID	Amino acid identity (%)
X. tropicalis	ABZ01809.1	92.6
Human	AAS86434.1	81.0
Rat	AAH89223.1	80.5
Mouse	NP_001103154.1	80.5
Puffer fish (*Tetraodon nigroviridis*)	CAG07017.1	52.9

xKazrinA interacts with xARVCF-catenin but not with Xp120-catenin

To determine whether the xARVCF–xKazrinA complex could be isolated from in vivo extracts, Myc-tagged xKazrinA was

Table 2. Comparison of xKazrin coiled-coil domain with related domains in other protein families

Protein domain	Identity/similarity (%)
FERM	23/48
SMC	25/48
HOOK	23/45
Myosin tail	20/40
SbcC	23/45

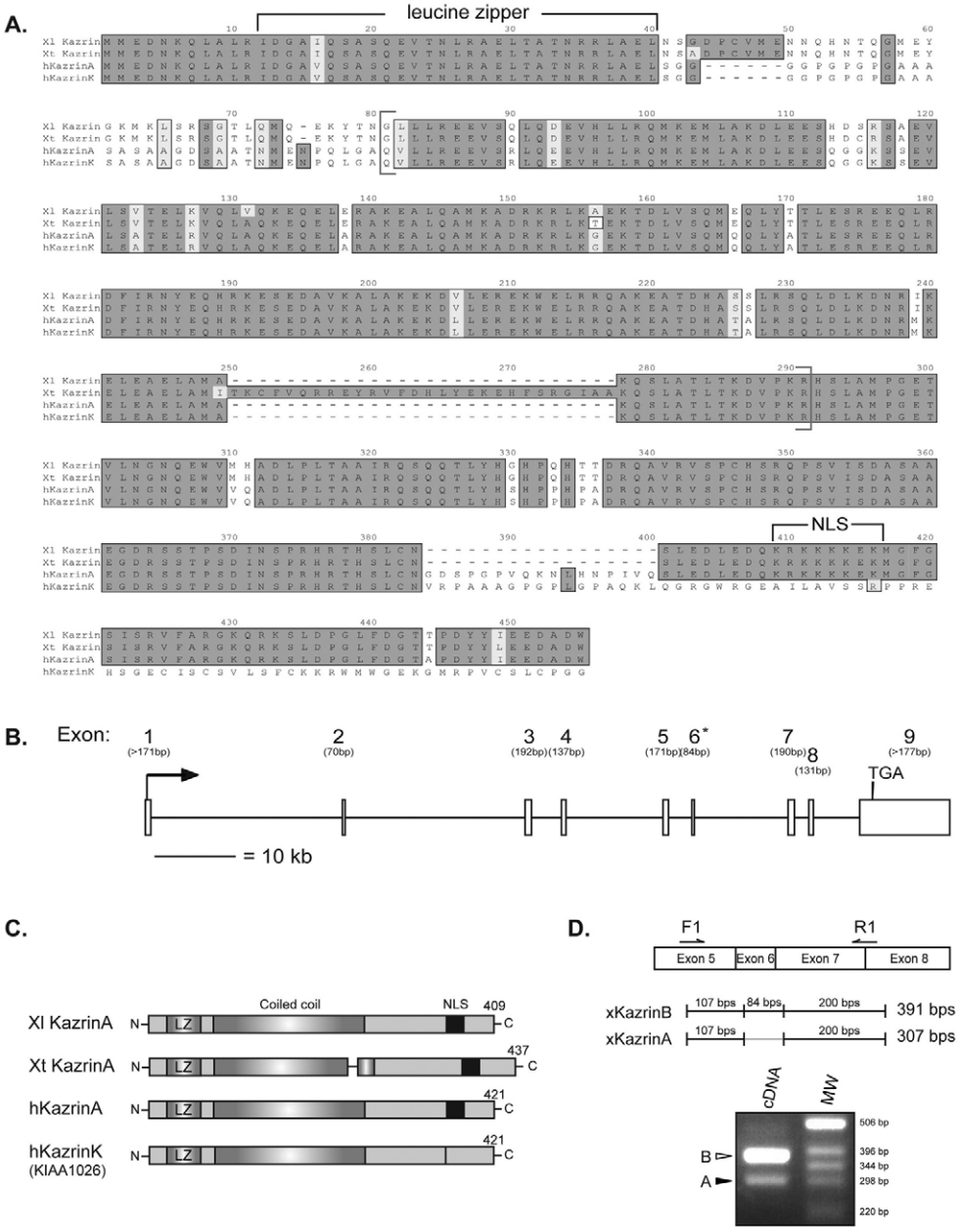

Fig. 1. Comparison of *Xenopus* and human Kazrin protein sequences. (**A**) Sequence alignment of *X. laevis* Kazrin (Xl Kazrin), *X. tropicalis* Kazrin (Xt Kazrin) and two isoforms of human Kazrin (hKazrinA and hKazrinK). Identical and similar residues are highlighted in black or grey, respectively. The central coiled-coil region (brackets), conserved potential leucine zipper and the predicted nuclear localization sequence (NLS) are indicated. (**B**) Genomic structure of *X. tropicalis* Kazrin. Genomic information was obtained from Ensembl database (Ensembl ID #ENSXETG00000013469 and scaffold 257). Asterisk indicates an alternatively spliced exon in *X. laevis*. (**C**) Comparison of *Xenopus* and human Kazrin isoforms. The coiled coil and polylysine tract (NLS) are respectively depicted as grey or black shaded areas. LZ indicates the putative leucine zipper region. Alternative splicing at the C-terminus of the human KazrinA isoform results in additional isoform human KazrinK without the polylysine tract. The total number of amino acids of each protein is indicated. (**D**) Identification of xKazrin isoforms using primers (F1 and R1) binding to the 5′- and 3′-flanking regions of exon 6. cDNA was synthesized from embryo stage 18 genomic RNA. Open arrowhead indicates PCR product of xKazrinB cDNA and closed arrowhead indicates that of xKazrinA. MW signifies molecular weight markers.

coexpressed in *Xenopus* embryos with HA-tagged xARVCF or HA-tagged Xp120. In agreement with our yeast two-hybrid results, coimmunoprecipitation assays showed that xKazrinA associates with xARVCF but not with Xp120-catenin (Fig. 2A).

To test whether xKazrin and xARVCF interact directly, each protein was purified as glutathione-*S*-transferase (GST)- or maltose-binding protein (MBP)-fusion constructs. Then, GST and MBP pull-down assays were performed (Fig. 2B, left versus right panels). GST–xKazrinA coimmunoprecipitated with MBP–xARVCF but not (or considerably more weakly) with MBP–Xp120, indicating specificity and a direct xARVCF–xKazrinA interaction. Using the same approach, *Xenopus* β-catenin (xβ-catenin) did not interact with xKazrinA (data not shown).

We further assayed for direct xARVCF–xKazrinA association using blot overlays (Fig. 2C) (Hall, 2004). Purified and immobilized GST–xKazrinA or GST were probed with purified MBP–xARVCF, MBP–Xp120 or MBP. A clear interaction was observed between membrane-bound GST–xKazrinA with MBP–xARVCF, although none was observed using MBP–Xp120 or MBP probes. Although cofactors might modulate their interaction in vivo, this data indicates that xARVCF and xKazrinA can selectively bind each other in vitro.

To outline the region interacting with xARVCF, we used GST–xKazrinA polypeptides representing the N-terminal, C-terminal, and coiled-coil regions of xKazrinA (GST–xKazrin NT, GST–xKazrin CT, and GST–xKazrin CC, respectively). Using a blot-overlay approach, these fusion proteins were assayed along with full-length GST–xKazrinA for association with MBP–xARVCF (Fig. 2D). xARVCF interacted with both full-length and coiled-coil GST–xKazrinA, but not with N-terminal or C-terminal fusions, suggesting that the central coiled-coil domain of xKazrin is required for xARVCF–xKazrin association.

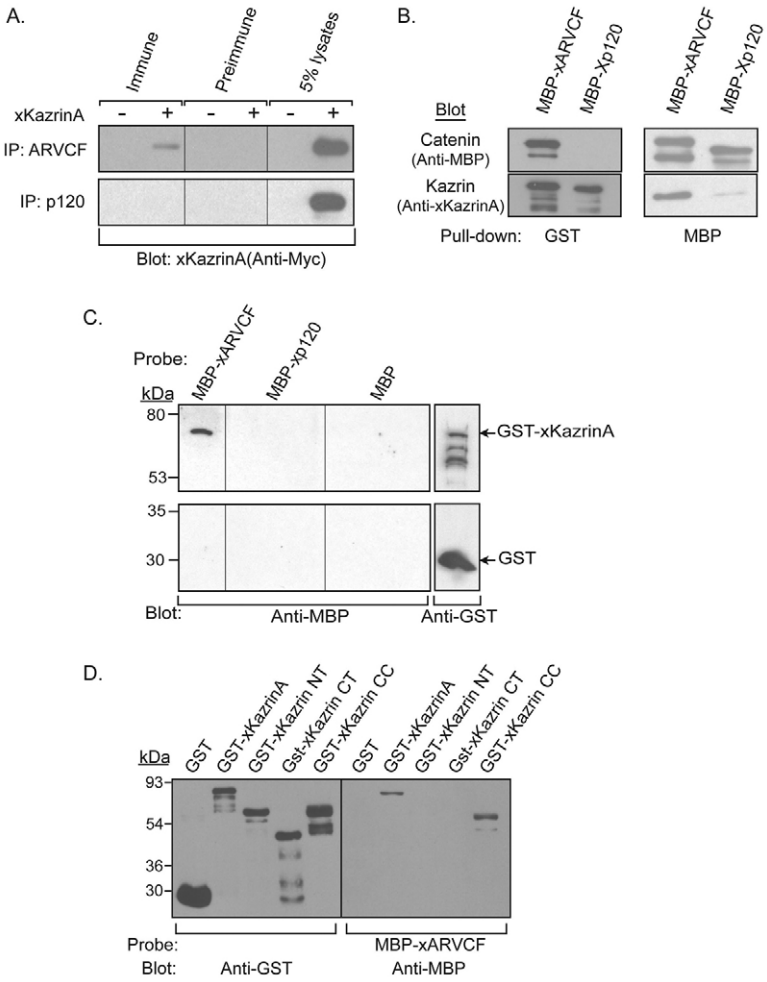

Fig. 2. Association of full-length xKazrinA with xARVCF. (**A**) *Xenopus* embryos expressing HA–xARVCF or HA–Xp120 with (+) or without (–) coexpressed Myc–xKazrinA were harvested at gastrula stage (stage 10.5). Lysates were immunoprecipitated using pre-immune, xARVCF or Xp120 polyclonal antisera, and interactions with xKazrinA detected by immunoblotting using anti-Myc antibody. Total lysates (5%) were also blotted. (**B**) In vitro co-precipitation of GST–xKazrinA with MBP–xARVCF. GST–xKazrinA was incubated with MBP–xARVCF or MBP–Xp120, precipitated using glutathione–agarose (left panels) or amylose–agarose (right panels) beads and the samples subjected to SDS-PAGE and immunoblotting using anti-MBP (top panels) or anti-Kazrin (bottom panels) antibodies. (**C**) Direct interaction of purified xARVCF with xKazrinA using blot overlay. Top panel: Duplicate lanes of purified GST–xKazrinA were electrophoresed and immobilized on nitrocellulose then probed using purified MBP–xARVCF, MBP–Xp120 or MBP. Protein complexes were then identified using anti-MBP antibodies (top-left panel). Presence of GST–xKazrinA was detected using anti-GST antibodies (top-right panel). As a negative control, purified GST was immobilized on nitrocellulose and processed in an identical manner (bottom panels). (**D**) Blot overlay of GST–xKazrinA deletion constructs. Purified GST–xKazrinA, GST–xKazrinA N-terminal (NT), GST–xKazrinA C-terminal (CT), GST–xKazrinA coiled-coil (CC), and GST proteins were electrophoresed and immobilized on nitrocellulose. Total loading was detected using anti-GST antibodies (left panel). The right panel was probed with MBP–xARVCF and the resulting protein complexes detected using anti-MBP antibodies.

xKazrinA associates with xARVCF within cells

To investigate the xARVCF–xKazrinA interaction within the physiological conditions provided by vertebrate cells, xARVCF-catenin or Xp120-catenin constructs were targeted to the mitochondrial outer membrane (MOM) via C-terminal fusion to the MOM localization domain of Bcl-X_L (Kaufmann et al., 2003; Waibler et al., 2001). Such xARVCF or Xp120 fusion proteins were localized to the MOM when expressed in *Xenopus* A6 kidney epithelial cells, resulting in a characteristic punctuate pattern (Fig. 3A). xKazrinA relocalized to the MOM when co-transfected with xARVCF–MOM but not with Xp120–MOM (Fig. 3B, top versus bottom panels). Similar patterns appeared when using human embryonic kidney (HEK-293) or human breast cancer cells (MCF-7) (data not shown). These experiments support the specificity and authenticity of the xARVCF–xKazrinA interaction within a cellular context.

Interaction domain mapping of the xARVCF–xKazrinA complex

To resolve xARVCF–xKazrinA interaction domains, deletion constructs were employed. Seven xKazrinA constructs were tested for interaction with xARVCF–MOM in A6 cells (Fig. 3C; supplementary material Fig. S3A). Deletion of the 70 N-terminal amino-residues of xKazrinA (Fig. 3C, MT xKazrin ΔN1) resulted in a construct similar to the C and D isoforms of human KazrinA (Groot et al., 2004), which retained competence to relocalize with xARVCF–MOM. Deletion of the N-terminal 175 amino acid residues (Fig. 3C, MT xKazrin ΔN2), or C-terminal 235 amino acids (Fig. 3C, MT xKazrin ΔC2) abolished xARVCF–xKazrinA association. A smaller C-terminal deletion of 127 amino acid residues (Fig. 3C, MT xKazrin ΔC1), as well as a more modest deletion of the C-terminal 47 amino acid residues of xKazrinA, inclusive of the NLS (Fig. 3C, MT xKazrin ΔNLSC), or mutation of the NLS (Fig. 3C, MT xKazrin NLSCm, see below), did not disrupt xARVCF–xKazrinA interaction. These data indicate that the region of xKazrinA necessary for interaction with xARVCF resides between amino acid residues 70–354, containing the coiled-coil domain of xKazrin up to the potential A/K isoform splice site at amino acid residue 354. This region is present in all identified isoforms of Kazrin (frog, human, mouse, rat and *Xenopus*), suggesting that ARVCF–Kazrin interactions might be shared. Indeed, as shown in supplementary material Fig. S9B, human KazrinE and KazrinK isoforms coimmunoprecipitate with xARVCF.

To map the interaction region(s) of xARVCF, we used MOM-targeted deletion constructs comprised of one or two of the three xARVCF domains (N-terminus, Arm domain and C-terminus; Fig. 3C and supplementary material Fig. S3B). When coexpressed with xKazrinA, only the full-length (Fig. 3C, HA xARVCFmom) and Arm–C-terminus (Fig. 3C, HA xARVCF-ACmom) constructs exhibited the capacity to relocalize xKazrinA to the MOM (supplementary material Fig. S3). xKazrin relocalization failed when using the isolated N- or C-terminal domains of xARVCF (Fig. 3C, HA xARVCF-Nmom or HA xARVCF-Cmom, respectively) [the latter binds ERBIN, ZO-1, ZO-2 and FRMPD2

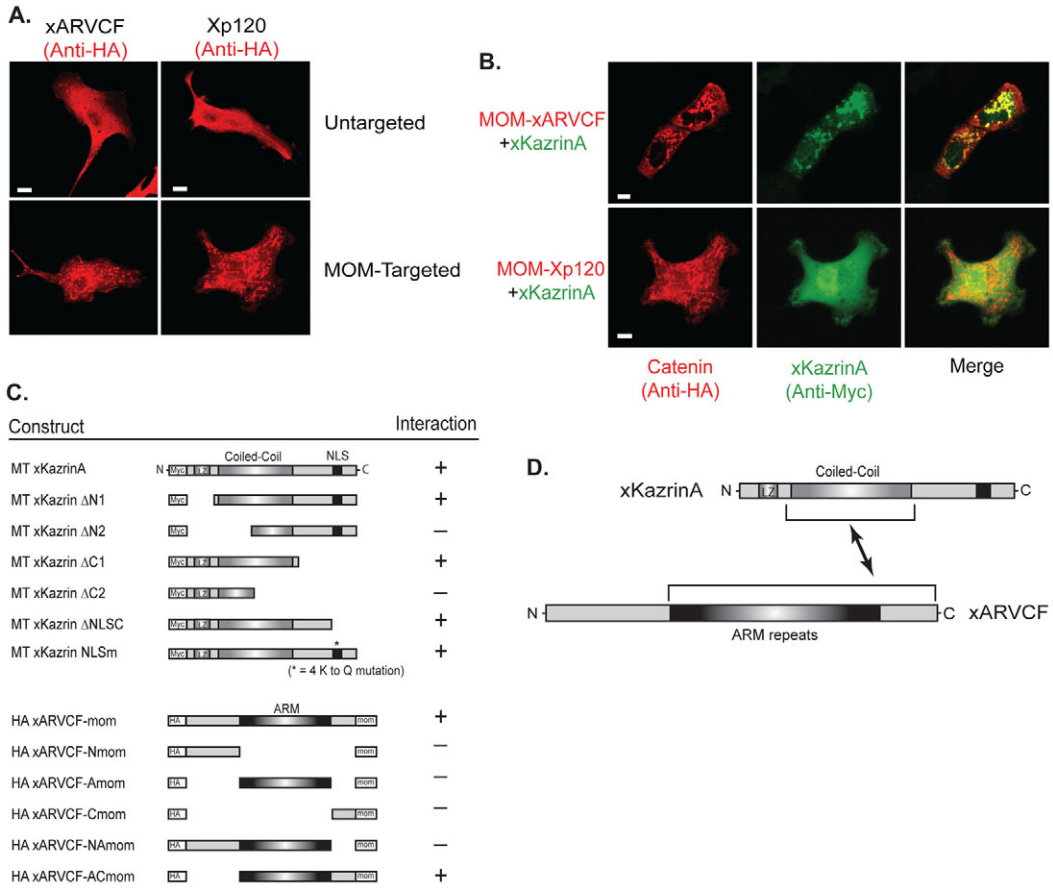

Fig. 3. Mitochondrial colocalization of xKazrinA with xARVCF in *Xenopus* A6 cells and binding domain mapping. (**A**) HA-tagged xARVCF or Xp120 were transfected into *Xenopus* kidney epithelial A6 cells, where they each displayed predominant cytoplasmic localization (top panels). Once fused to a peptide sequence tag from human Bcl-Xl directing their ectopic localization to the MOM, xARVCF and Xp120 displayed a punctate pattern characteristic of mitochondrial localization (bottom panels). (**B**) Coexpression of Myc–xKazrinA with MOM-targeted HA–xARVCF or HA–Xp120 (top and bottom panels, respectively). Cells were coimmunostained for localization of the catenin (HA-epitope, left panels) and for xKazrinA (Myc-epitope, center panels). Co-localization of xKazrinA was observed with xARVCF but not with Xp120, as shown in the merged images (right panels). (**C**) List of Myc-tagged (MT) xKazrinA and HA-tagged xARVCF constructs (see text for details) and their interaction status. Asterisk indicates mutation of lysine to glutamine; LZ, leucine zipper; mom, mitochondrial outer membrane; ARM, Armadillo domain. The co-relocalization of xKazrinA deletion mutants was tested in the presence of full-length MOM-targeted xARVCF (upper set). Conversely, full-length xKazrinA was tested for co-relocalization with deletion constructs of MOM-targeted xARVCF (lower set). A positive score (+) indicates that numerous cells coexpressing the indicated xKazrinA or xARVCF deletion constructs showed colocalization of xKazrinA with the MOM-targeted xARVCF construct. (**D**) Representation of the xARVCF–xKazrinA interaction, indicating the putative regions of association. Scale bars: 20 μm.

(Kausalya et al., 2004; Laura et al., 2002; Stenzel et al., 2009)]. Relocalization also failed when using the xARVCF Arm domain (Fig. 3C, HA xARVCF-Amom), or upon removal of the xARVCF C-terminus (Fig. 3C, HA xARVCF-NAmom). These data collectively indicate that a region(s) comprised of the Arm and C-terminal domains of xARVCF is required for interaction with the coiled-coil domain of xKazrin (Fig. 3D).

xKazrinA and xARVCF colocalize at cell–cell contacts in *Xenopus* blastula ectoderm

To assess xKazrin intracellular distribution in *Xenopus* tissue, immunofluorescence was performed of *Xenopus* blastula ectoderm (animal caps) expressing Myc–xKazrinA. Most xKazrinA protein was present at cell–cell borders, with some staining evident in the nucleus (data not shown). The nuclear presence of Kazrinin in vivo is in accordance with its nuclear localization in cell lines and human skin (supplementary material Fig. S1) (Nachat et al., 2009; Sevilla et al., 2008a).

To assess HA–xARVCF and Myc–xKazrinA colocalization following coexpression in vivo, immunofluorescent images were acquired from the outer ectodermal cell layer at blastula stages. Colocalization occurred along cell–cell borders in the *X*–*Y* plane (Fig. 4A–C), and to a significant if not complete extent along the *Z*-axis (Fig. 4D). In general, these findings are consistent with the biochemical association of xARVCF and xKazrinA.

The xARVCF–xKazrinA complex is not a core component of adherens junctions or desmosomes

Because xARVCF directly binds cadherin juxtamembrane regions (Kaufmann et al., 2000; Mariner et al., 2000; Paulson et al., 2000), we tested whether xKazrinA and xARVCF colocalize with C-cadherin, a major cadherin essential for *Xenopus* early development (Heasman et al., 1994; Lee and Gumbiner, 1995). *Xenopus* C-cadherin (xC-cadherin) colocalized at cell–cell borders with xKazrinA as well as with xARVCF (Fig. 4E–L), consistent with a possible association of xKazrinA with adherens junction components.

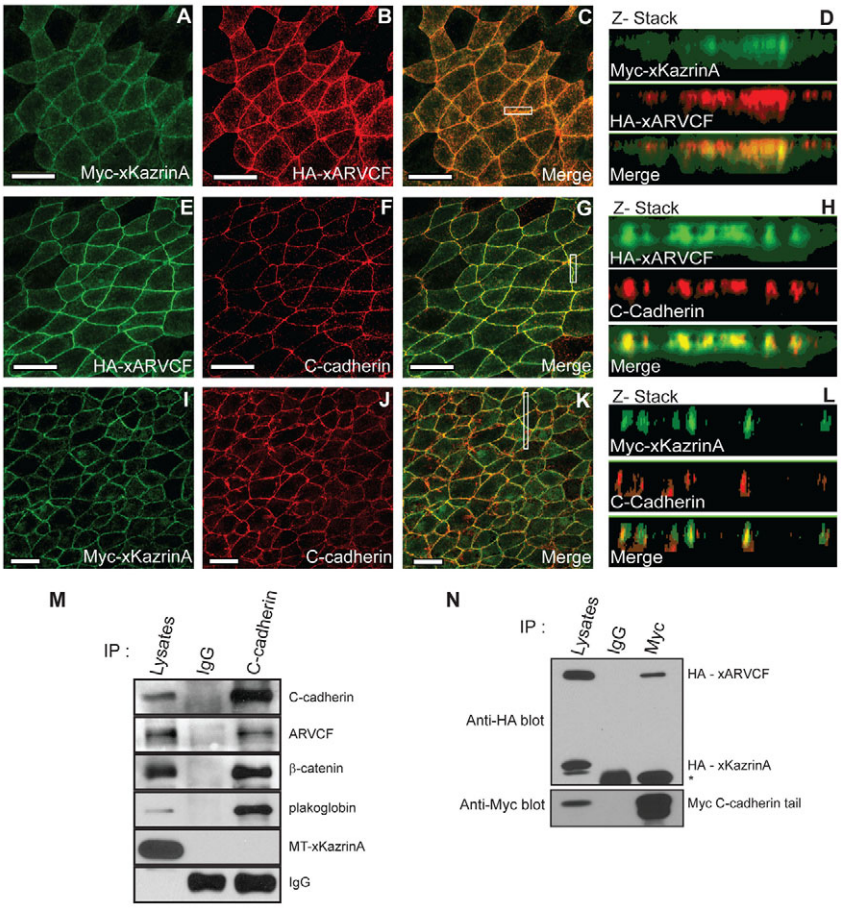

Fig. 4. Cellular localization of xKazrinA in ectodermal explants of *Xenopus* blastula (stage 10) embryos. (**A–D**) Localization and colocalization of coexpressed Myc–xKazrinA and HA–xARVCF in the outer ectodermal layer, detected using anti-Myc and anti-HA antibodies, respectively. The area outlined by a white rectangle in C, was viewed using *Z*-stack section images (shown in D). (**E–H**) Localization and colocalization of HA–xARVCF and C-cadherin, detected using anti-Myc and anti-C-cadherin antibodies, respectively. (**I–L**) Localization and colocalization of Myc–xKazrinA and xC-cadherin. (**M**) Co-immunoprecipitation of Myc–xKazrinA (MT-xKazrinA) with adherens junction components. Myc–xKazrinA was expressed in early embryos lysed at stage 9–10 and endogenous xC-cadherin was immunoprecipitated. Co-precipitated proteins were detected by immunoblotting using the indicated antibodies. (**N**) Co-immunoprecipitation tests following the coexpression of Myc–xC-cadherin tail, HA–xARVCF and HA–xKazrinA. Myc–xC-cadherin tail was precipitated using anti-Myc antibodies. Co-associated HA–xARVCF and HA–xKazrinA were detected (versus not) using anti-HA antibody. Asterisk indicates migration of IgG heavy chains (50 kDa). Scale bars: 50 µm.

To test whether xKazrinA and C-cadherin form a larger complex, presumably bridged by xARVCF, we overexpressed Myc–xKazrinA followed by C-cadherin immunoprecipitation and western blotting (Fig. 4M). As anticipated, endogenous C-cadherin co-precipitated endogenous xARVCF, as well as *Xenopus* β-catenin and plakoglobin. Importantly, however, it did not co-precipitate Myc–xKazrinA. In further tests, we simultaneously overexpressed three components: HA–xKazrinA, HA–xARVCF and the cytoplasmic tail of C-cadherin (Myc-tagged). Whereas xARVCF coimmunoprecipitated with the cytoplasmic domain of C-cadherin as expected, HA–xKazrinA was not present in conjunction with cadherin (Fig. 4N). Furthermore, we could not detect an interaction between xKazrinA and xC-cadherin following chemical crosslinking [using DTSSP; 3,3′-dithiobis(sulfosuccinimidyl propionate)] (data not shown). These results indicate xC-cadherin–xARVCF association as anticipated, but given our coimmunoprecipitation results, not cadherin association with xKazrinA.

Because Kazrin associates with envoplakin and periplakin at desmosomal or interdesmosomal regions in human keratinocytes (Groot et al., 2004), and ARVCF- and p120-catenins have been reported at desmosomes (Borrmann et al., 2006; Johnson and Boekelheide, 2002; Kanno et al., 2008a; Kanno et al., 2008b), we wanted to know whether ARVCF is resident at desmosomes in human keratinocytes. As shown in Fig. 5, both Myc–xARVCF and human Kazrin partially colocalized with the desmosomal marker desmoplakin (Fig. 5A–C and Fig. 5D–F, respectively), and with desmoglein3 in human keratinocytes (Fig. 5G–I). We then employed transmission EM, but in our hands this did not further clarify ARVCF or Kazrin presence at desmosomes and/or adherens junctions (data not shown).

To further probe desmosomal associations, we turned to biochemical precipitations from *Xenopus* embryo (Fig. 5J) and human epithelial carcinoma cell extracts (A431) (Fig. 5K). The cytoplasmic tail of human desmoglein1 (Fig. 5J) or full-length desmoglein1 (Fig. 5K) failed to co-precipitate *Xenopus* or human ARVCF from either system. Plakoglobin and C-cadherin were positive controls for the respective binding functionality of desmoglein and ARVCF in *Xenopus* embyos (Fig. 5J). As evaluated by these criteria, our data do not support xARVCF as being a core component of the desmosome.

xKazrinA and xARVCF form a complex with the xβ2-spectrin cytoskeletal protein

To further address how the xARVCF–xKazrinA complex localizes to junctional areas, we performed yeast two-hybrid screening of xKazrinA to identify novel binding partners (Hybrigenics). From an adult mouse brain cDNA library, we obtained 64 positive clones (partial list in supplementary material Table S1). Notably, nine clones encoded plasma-membrane-associated proteins. These included two p120-catenin subfamily members (δ-catenin and p0071), the tight junction protein symplekin (Keon et al., 1996), the spectrin binding protein Camsap1 (Baines et al., 2009; Yamamoto et al., 2009), and three spectrin family members (α1-, α2- and β2-spectrins) (for a review, see Bennett and Healy, 2009). This screen was not saturating because we did not isolate ARVCF-

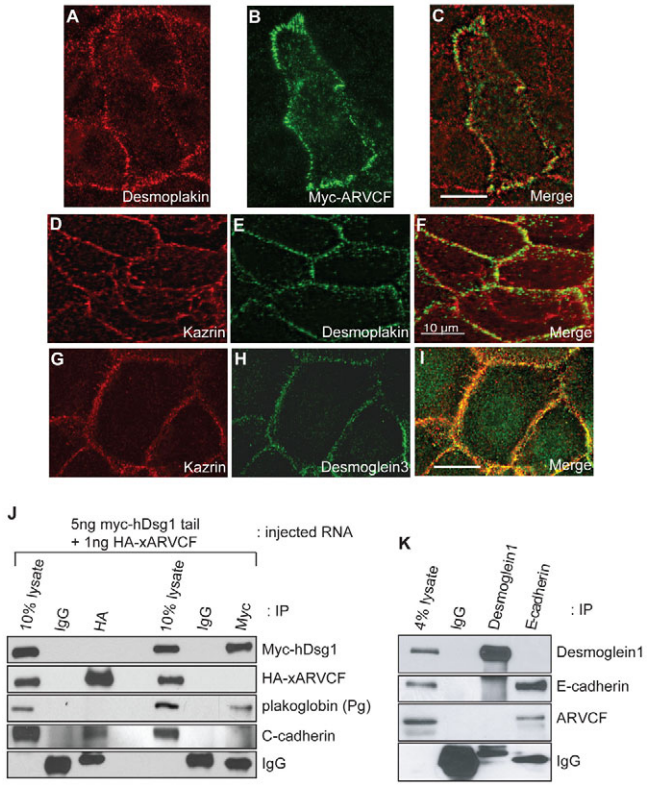

Fig. 5. Kazrin and ARVCF localization in desmosome. (**A**–**I**) Human keratinocytes were immunolabeled for the endogenous desmosomal marker desmoplakin (A,E), Myc-tagged xARVCF (B), or endogenous Kazrin (D,G). In addition, Kazrin localization was compared to that of endogenous desmoglein3 (H), a desmosomal cadherin. Merged images (F,I) show partial colocalization of Kazrin with desmoplakin and extensive colocalization with desmoglein3. Colocalization between desmoplakin and ARVCF is shown in C. Photos represent projection images of deconvolved *Z*-stacks. Scale bars: 10 μm. (**J**) Interaction between desmosomal cadherin desmoglein1 (Dsg1) and xARVCF in *Xenopus* embryo lysates. Indicated amounts of in vitro transcribed RNAs were microinjected into one-cell stage embryos. Then, early gastrula embryos were lysed and human desmoglein1 tail or xARVCF were immunoprecipitated, followed by SDS-PAGE and western blotting. (**K**) Endogenous desmoglein1 or E-cadherin were immunoprecipitated from confluent A431 human epithelial carcinoma cells. Bound endogenous ARVCF was detected with human ARVCF-specific antibody.

catenin, envoplakin or periplakin. Contributing factors could be lower ARVCF expression in mammals than in amphibians (Mariner et al., 2000), and little envoplakin or periplakin presence in neural tissues (Aho et al., 1998).

Spectrin as a potential Kazrin-binding partner was intriguing given that our earlier structural analysis of xKazrinA predicted its coiled-coil domain to be similar to the spectrin-repeat region of α-spectrin (GenThreader program in PSIPRED Protein Structure Prediction Server; http://bioinf.cs.ucl.ac.uk/psipred/; *P*-value = 4e–04) (Jones et al., 1999). In mammals, there are two α-spectrin genes and five β-spectrin genes. Their gene products form αβ-heterodimers that orient end-to-end to form $\alpha_2\beta_2$-tetramers. Tetramers in turn interact with microfilaments, neighboring spectrin tetramers, and other proteins such as band 4.1, ankyrin, adducin and calmodulin, forming a cytoskeletal web that functions in many contexts (for a review, see Bennett and Healy, 2009). Anchoring points, such as provided by band 4.1 and ankyrin, facilitate the plasma membrane association of the spectrin cytoskeleton, as do junctional cadherins (see later) (Bennett and Healy, 2009). In *Xenopus*, two spectrins are known, α-spectrin (also known as α-fodrin) and β-spectrin (Giebelhaus et al., 1987; Klein et al., 2002). *Xenopus* α-spectrin (xα-spectrin), although highly expressed in oocytes, becomes reduced following fertilization (Giebelhaus et al., 1987), whereas xβ-spectrin-encoding mRNA is expressed throughout development, as assessed via semiquantitative RT-PCR (supplementary material Fig. S4B).

We wondered whether the spectrin network might be relevant to xARVCF–xKazrinA localization to cell–cell borders. Confocal microscopy and biochemical approaches were employed using a partial xβ2-spectrin cDNA (GenBank #BC046267.1). This construct is the longest available xβ-spectrin, and is homologous to human β2-spectrin isolated from our yeast two-hybrid screen (74.6% identical). It encodes the N-terminal actin-binding domain of β2-spectrin (ABD; which binds band 4.1 and adducin), and five spectrin repeats (Fig. 6A and supplementary material Fig. S4A). Isolation of shorter yeast clones from our two-hybrid screen suggested that the β1- or β2-spectrin regions extending from the end of the second spectrin repeat to the middle of the third repeat are sufficient to bind Kazrin (data not shown).

The xKazrinA–xβ2-spectrin interaction was supported using co-precipitation tests of *Xenopus* embryo lysates in which full-length xKazrinA and partial xβ2-spectrin proteins were coexpressed (Fig. 6B). Furthermore, using confocal microscopy, xKazrinA and xβ2-spectrin colocalized as expected to cell–cell borders in blastula ectoderm (Fig. 6C). To test whether xβ2-spectrin binds to the xARVCF–xKazrinA complex in vivo, varying amounts of spectrin were expressed in *Xenopus* embryos with a constant amount of xKazrinA, and the endogenous xARVCF complexes isolated and assayed (Fig. 6D). xβ2-spectin as well as xKazrinA co-precipitated with xARVCF. Because xβ2-spectrin expression did not alter xARVCF–xKazrinA co-precipitation, we expect that a ternary xARVCF–xKazrinA–xβ2-spectrin complex was formed. However, because a prior study reported association of β2-spectrin with E-cadherin (through ankyrin) (Kizhatil et al., 2007), it was conceivable that xARVCF association with xβ2-spectrin occurred via their mutual association with cadherin. We tested this possibility using co-precipitation assays. As shown in Fig. 6E, xARVCF but not xC-cadherin associated with xβ2-spectrin and xKazrinA. Thus, the ARVCF–Kazrin complex probably associates with spectrin through Kazrin binding to spectrin.

xARVCF partially rescues embryonic phenotypes resulting from xKazrin depletion

Morpholino-directed Kazrin depletion in early *X. tropicalis* embryos was previously reported to result in ectodermal blistering, as well as a shortened body axis, head reductions and somitic defects (Sevilla et al., 2008b). Because the mRNA sequence targeted by the *X. tropicalis* morpholino is completely conserved with that in *X. laevis*, we used *X. tropicalis* morpholino (KMO1) in our study, and demonstrated its efficacy in blocking in vitro translation of Kazrin-encoding mRNA, and in knocking-down *X. laevis* Kazrin to 60% of endogenous levels by neurulation stages (significant maternal protein loading precluded obtaining earlier effects) (supplementary material Fig. S6A and Fig. S6B, respectively). The phenotypes appearing in *X. laevis* were similar to those previously indicated in *X. tropicalis* (Sevilla et al., 2008b). However, Kazrin depletion in *X. laevis* appeared to have a more severe impact upon the ectoderm, as evident in abnormal

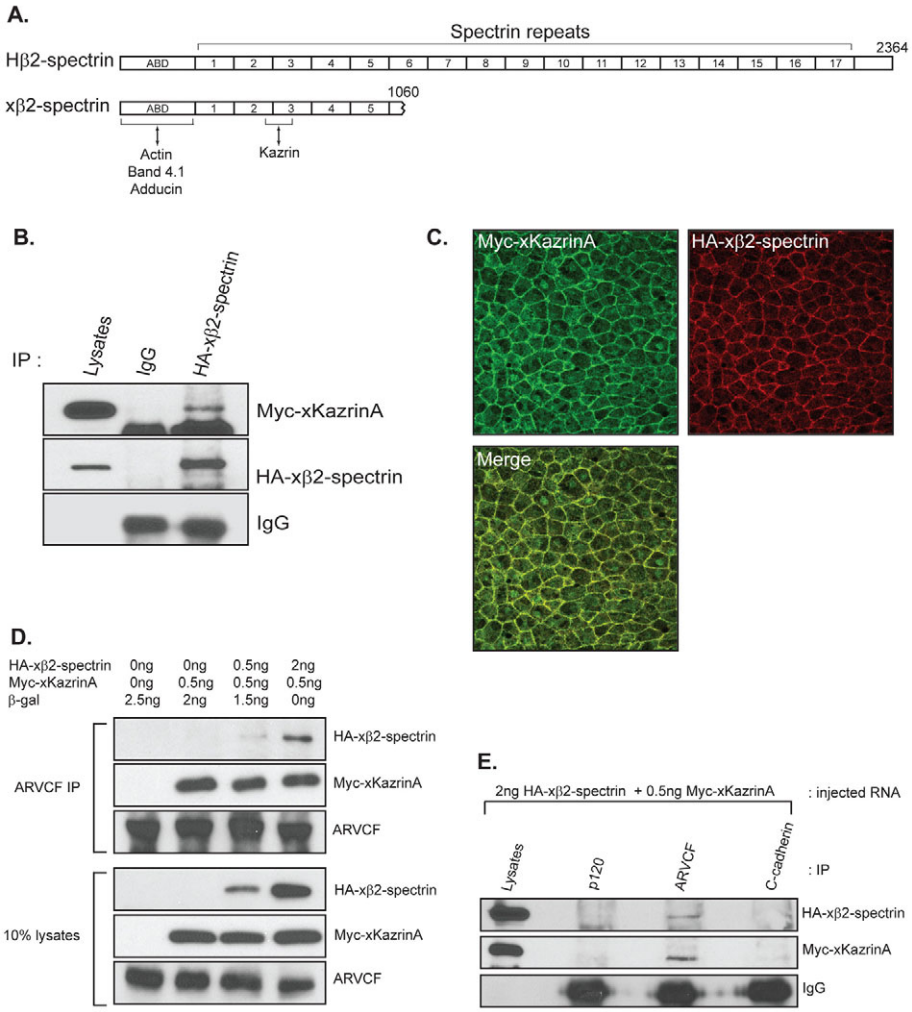

Fig. 6. Association of xKazrinA and xβ2-spectrin, and ternary complex formation with xARVCF. (**A**) Comparison of human β2-spectrin (gene bank ID # NM_003128) and *Xenopus* partial β2-spectrin (BC046267). Actin-binding domain (ABD) and putative Kazrin-binding region are depicted. (**B**) In vivo binding of xKazrinA and xβ2-spectin. Enzymatically synthesized mRNAs encoding Myc–xKazrinA and HA–xβ2-spectrin were co-injected into one-cell stage embryos, and the blastula embryo lysates were HA-immunoprecipitated followed by Myc immunoblotting. (**C**) Colocalization of xKazrinA and xβ2-spectrin in blastula ectoderm. Animal caps were isolated from blastula embryos (stage 9–10) expressing Myc–xKazrinA and HA–xβ2-spectrin, followed by their respective (Myc and HA) immunofluorescent detection. (**D**) Formation of xARVCF, xβ2-spectrin and xKazrinA ternary complex. Blastula lysates from embryos injected with indicated amounts of each mRNA were immunoprecipitated with xARVCF antibody, followed by immunoblotting for Myc–xKazrinA and HA–xβ2-spectrin. (**E**) ARVCF-specific ternary complex. Lysates from embryos expressing xβ2-spectrin and xKazrinA were immunoprecipitated using the indicated antibodies. Co-precipitating xβ2-spectrin or xKazrinA were detected by immunoblotting.

neural tube closure during neurulation (supplementary material Fig. S6C, upper panels), and in regional ectoderm shedding in addition to blistering (noted previously) at early tailbud stages (supplementary material Fig. S6C, bottom panels and Fig. 7A, middle panel). The fraction of embryos exhibiting such phenotypes increased in a dose-dependent manner (supplementary material Fig. S6D). Because we obtained the same results using an independent non-overlapping Kazrin morpholino in *X. laevis*, the specificity of our phenotype was supported (data not shown). To test for an in vivo functional interaction between xARVCF and xKazrinA, we attempted to rescue ectodermal shedding through ectopic expression of xARVCF (Fig. 7, Table 3). As shown in Fig. 7B, Kazrin depletion was partially rescued by an appropriately titrated dose of ectopic xARVCF (dose subphenotypic in isolation), consistent with xKazrin–xARVCF functional interactions in maintaining ectodermal integrity.

Kazrin depletion decreases cadherin protein levels and cell–cell attachment

Our data suggested that xKazrinA and xARVCF form a complex that is capable of associating with spectrin, and furthermore that the xKazrinA–xARVCF complex participates in maintaining ectodermal integrity. However, it remained unclear at the mechanistic level how xKazrinA depletion alters ectodermal integrity. Given their established contributions to cell adhesion, we first considered the effects upon C-cadherin and E-cadherin. Interestingly, the levels of both cadherins were decreased after xKazrin depletion (Fig. 8A), as was that of desmoglein1, a desmosomal cadherin (supplementary material Fig. S5). A previous report employing cell lines used immunofluorescence to indicate that Kazrin overexpression lowers desmoplakin and perhaps E-cadherin levels (Sevilla et al., 2008a). Intriguingly, both in our and others' hands (Sevilla et al., 2008b) (data not shown), Kazrin overexpression in *Xenopus* does not generate an obvious phenotype(s). Although speculative, it is possible that effects occur but are more effectively compensated for in vivo than in vitro. To evaluate xKazrin depletion effects on cell–cell adhesion in a more controlled setting, we performed cell dissociation and cell re-aggregation assays using blastula ectoderm tissue (animal caps). xKazrin-depleted tissue exhibited accelerated dissociation compared to controls (Fig. 8B) and, correspondingly, they experienced delayed reaggregation (data not shown). Considering the key roles of cadherins in determining the outcome of such dissociation–reaggregation assays (Turner et al., 1992), together with our biochemical evidence, the observed reduction of ectoderm integrity is probably due to reduced cadherin levels following xKazrin depletion. In support of this proposition, xKazrin depletion phenotypes were partially rescued upon ectopic expression of an appropriately titrated dose of C-cadherin (subphenotypic in isolation)

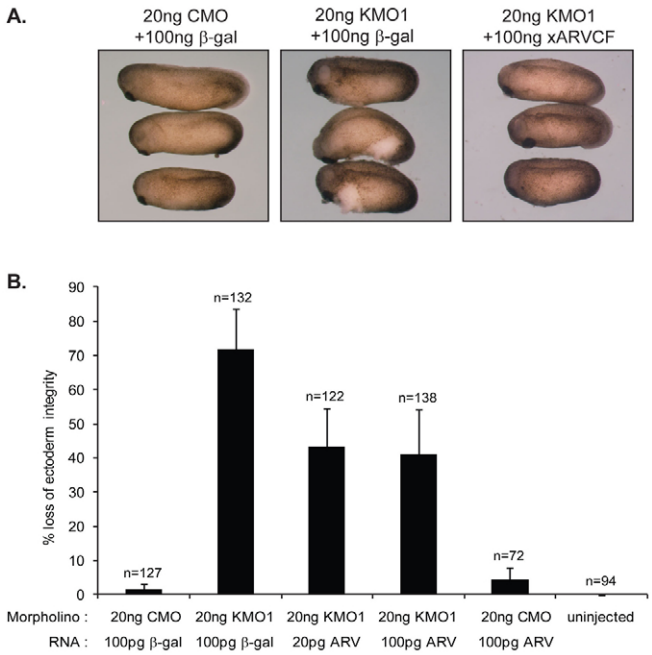

Fig. 7. Rescue of loss of ectoderm integrity, induced upon xKazrin depletion, through ectopic expression of xARVCF. (**A**) The indicated morpholinos and mRNAs were co-injected into one-cell stage embryos. After vitelline membrane removal, representative tailbud stage embryos were imaged (stage 20–22). (**B**) xARVCF rescue of xKazrin depletion effects upon ectoderm integrity. Two concentrations of xARVCF-encoding mRNA (ARV) were used in the rescues, with similar results being observed from four independent experiments. Error bars represent standard error of the mean (s.e.m.). Numerical results are shown in Table 3.

(Fig. 8C). Together, our in vivo data suggests that Kazrin positively modulates cell–cell contacts, with the xARVCF–xKazrinA complex probably being pertinent to effects upon cadherin levels.

Kazrin depletion leads to increased RhoA activity and cortical actin disorganization

A remaining issue was how xKazrinA, or the xARVCF–xKazrinA complex, modulates cadherin stability. p120 subfamily catenins including ARVCF are thought to stabilize cadherins by binding cadherin membrane-proximal domains and blocking certain protein associations (such as with Hakai or presenilin-1) (Baki et al., 2001; Fujita et al., 2002; Marambaud et al., 2002), that would otherwise promote cadherin degradation and/or endocytosis (Davis et al., 2003; Ireton et al., 2002; Xiao et al., 2003). Regulation of Rho-GTPases by p120 subfamily catenins is further relevant to cadherin stabilization and/or endocytosis (Akhtar and Hotchin, 2001; Charrasse et al., 2006; Izumi et al., 2004; Lamaze et al., 1996; Leung et al., 1999) (for a review, see Anastasiadis, 2007; Xiao et al., 2007). Interestingly, a non-biased screen earlier correlated Kazrin overexpression with inhibition of clathrin-mediated endocytsosis of transferrin receptor (Schmelzl and Geli, 2002). Thus, Kazrin together with p120 subfamily catenins might be relevant to cadherin endocytosis. Indeed, cadherin levels after Kazrin depletion were restored when embryos were incubated with a specific dynamin inhibitor (Dynasore; Fig. 8D) (Macia et al., 2006), and ectodermal defects were partially rescued in parallel (data not shown). This suggests a potential role of Kazrin in cadherin endocytosis, although we never resolved Kazrin in complex with cadherin using standard immunoprecipitation (Fig. 4M,N) or chemical crosslinking (using DTSSP, data not shown). Furthermore, although less compelling, we never observed that association of xARVCF with cadherin was altered by xKazrinA expression (data not shown).

In common with cadherin, the level of xARVCF, Xp120 and xβ-catenin became decreased in response to xKazrin depletion (data not shown). One possible explanation for the modulation of cadherin protein levels by Kazrin is its above-shown relationship with ARVCF. On the basis of published reports, lowered ARVCF (as for p120) levels are expected to result in lowered cadherin levels (Davis et al., 2003; Fang et al., 2004; Ireton et al., 2002; Xiao et al., 2003). Symmetrically, lowered cadherin presence can result in reduced catenin levels (e.g. of β-catenin) (Papkoff, 1997; Thoreson et al., 2000). At this time, we do not know the temporal hierarchy of events following Kazrin perturbation that result in altered levels and/or functions of cadherin–catenin complex components. This will require further study.

Nonetheless, given the known effects of ARVCF-catenin (and p120-catenin) on small GTPases (Anastasiadis et al., 2000; Fang et al., 2004; Grosheva et al., 2001; Noren et al., 2000), we turned our attention to xKazrinA effects on RhoA and Rac, and on cortical actin organization in plasma-membrane regions. We initially evaluated RhoA activity in embryos following the depletion of xKazrin and/or xARVCF (Fig. 8E). Interestingly, xKazrin depletion significantly increased RhoA activity, an effect likewise observed (and expected) following xARVCF knockdown (Fang et al., 2004). Coordinate xKazrin and xARVCF depletions had an additive effect on RhoA activity, as seen by comparing 10 ng deliveries of each morpholino (Fig. 8E, lane 6 versus 2 and 4). Because Rac1 was not affected by xKazrin depletion (data not shown), Kazrin might be a RhoA-specific modulator. Our results are in line with a report indicating that Kazrin overexpression inhibits RhoA in human keratinocytes, with no apparent effect on Rac1 (Sevilla et al., 2008a). Thus, although Kazrin and xARVCF appear to have shared inhibitory effects on

Table 3. xARVCF rescue of xKazrin depletion

Injection		Number of embryos			
Morpholino	RNA	Total (*n*)	Normal	Reduced tissue integrity	Number of experiments
20 ng CMO	100 pg β-gal	127	123	2	4
20 ng KMO1	100 pg β-gal	132	26	97	4
20 ng KMO1	20 pg xARVCF + 80 pg β-gal*	122	67	43	4
20 ng KMO1	100 pg xARVCF	138	75	61	4
20 ng CMO	100 pg xARVCF	72	69	3	2
Uninjected	Uninjected	94	94	0	4

CMO, control morpholino; KMO1, *X. Laevis* morpholino. *80 pg of β-galactosidase mRNA was co-injected with 20 pg xARVCF mRNA to equalize the total amount of injected mRNA.

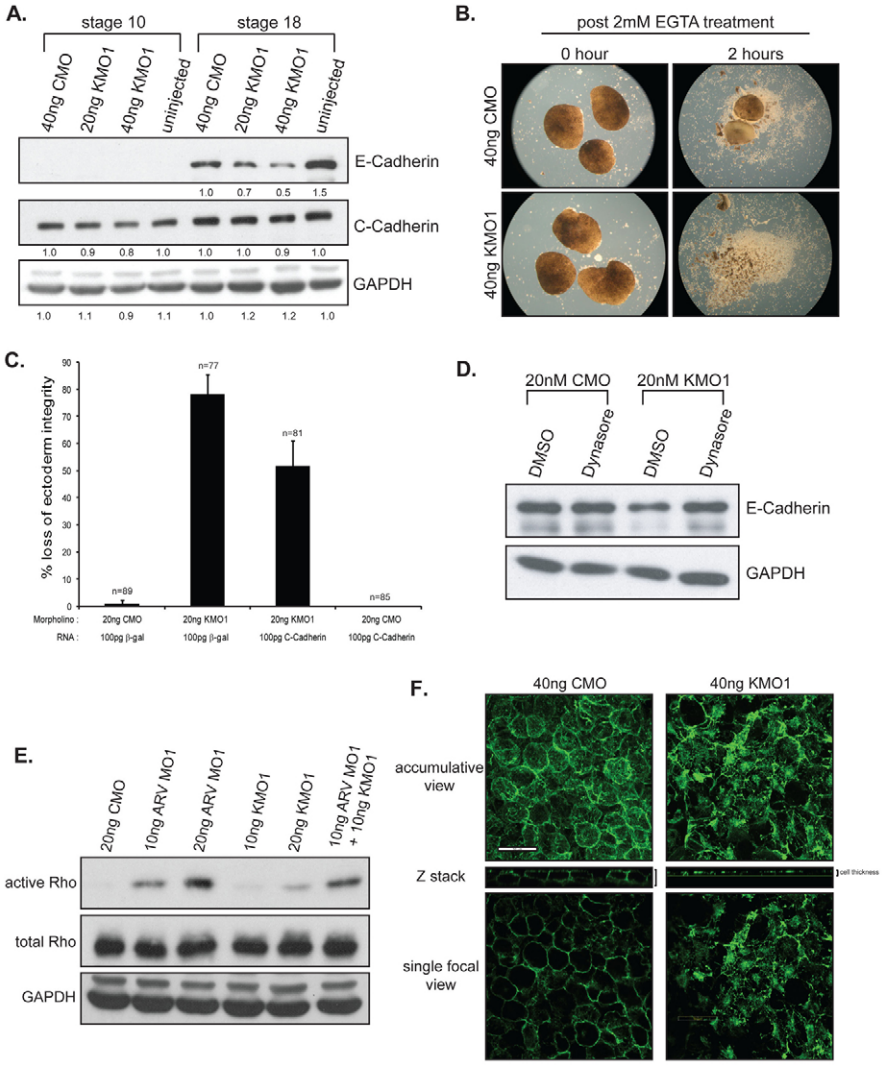

Fig. 8. Effects of xKazrin depletion on cadherin expression, cell–cell adhesion, Rho activity and actin organization. (**A**) Decrease of cadherin protein levels after xKazrin depletion. Embryos injected at the one-cell stage with different amounts of the indicated morpholinos were lysed at early gastrula (stage 10) and neurula (stage 18) stages. xE-cadherin and xC-cadherin levels were visualized by immunoblotting. Band intensity was measured with AlphaEaseFC software (Alpha Innotech Corporation). (**B**) Cell dissociation assay using animal cap explants. Blastula ectoderm (animal caps; stage 9–10) from embryos injected with CMO or KMO1 were dissociated in the presence of 2 mM EGTA. Photos were taken at 0 hour and 2 hours following EGTA addition. (**C**) Rescue of ectodermal integrity, reduced upon xKazrin depletion, through expression of xC-cadherin. Embryos injected with the indicated morpholino and mRNA were assessed for ectoderm shedding at tailbud stages (stage 20–22). Error bars represent standard error of the mean (s.e.m.). Numerical results are shown in supplementary material Table S2. (**D**) Effect of inhibiting clathrin-mediated endocytosis on the reduced xE-cadherin levels observed following xKazrin depletion. One-cell stage embryos were injected with the indicated morpholinos. Embryos were subsequently (32–64 cell stages) incubated with 50 mM Dynasore (versus DMSO solvent). Lysates from neurula (stage 18) embryos were immunoblotted for xE-cadherin and GAPDH. (**E**) Rho activity in response to xARVCF and/or xKazrin depletion. The indicated morpholinos were injected into one-cell stage embryos, and lysates from late blastula (stage 9–10) embryos were tested for Rho activity in vitro. (**F**) Actin staining of blastula ectoderm after Kazrin depletion. Animal cap were isolated as mentioned in B and filamentous actin in deep (inner) cells was visualized using phalloidin-Alexa 488 fluorescence. Scale bar: 50 µm.

RhoA, one distinction (relative to ARVCF and related p120 subfamily members) is that Kazrin is not likely to modulate Rac1 in this context (Anastasiadis et al., 2000; Fang et al., 2004; Grosheva et al., 2001; Noren et al., 2000). Because RhoA activation might have contributed to the ectoderm fragility we observed following Kazrin depletion, we tested the rescuing capacity of carefully titrated dominant-negative RhoA (versus dominant-active RhoA), upon co-injection with KMO1. In line with RhoA being functionally relevant and possibly downstream of Kazrin, co-injection of dominant-negative RhoA mildly rescued observed phenotypes, whereas titrated dominant-active RhoA doses only worsened developmental defects (data not shown).

Because ectopic RhoA activation modulates actin and cell structure and/or cell morphology (Paterson et al., 1990), we employed phallodoin staining to grossly resolve Kazrin-depletion effects on actin organization in embryos (Fig. 8F). Whereas control embryos exhibited a defined enrichment of cortical actin at cell–cell borders, Kazrin-depleted embryos displayed a disorganized pattern and an actin signal of reduced thickness along the *Z*-axis (Fig. 8F). The cytoskeletal disorganization we resolved in vivo appears to be in keeping with a previous report employing keratinocytes (Sevilla et al., 2008a). In summary, Kazrin appears to be a negative regulator of RhoA in vivo, suggesting that increased RhoA activity upon Kazrin depletion contributes to microfilament reorganization, and possibly to lowered cadherin levels and ectodermal integrity as previously noted (Charrasse et al., 2006; Leung et al., 1999).

xKazrinA interacts with Xp190B RhoGAP

We wondered whether Kazrin might modulate RhoA via another protein(s), because predictive analysis suggested that Kazrin was unlikely to directly bind RhoA. Common modulators of RhoA include Rho GDIs (Rho GDP dissociation inhibitors), RhoGAPs (Rho GTPase activation proteins) and Rho GEFs (Rho guanine nucleotide exchange factors). Intriguingly, from our xKazrinA yeast two-hybrid screen, we identified multiple independent clones of mouse p190B RhoGAP (supplementary material Table S1). This novel Kazrin interaction suggested one means by which it might influence RhoA activity and function.

There are two p190 RhoGAPs, p190A and p190B, and both are widely functioning negative regulators of Rho GTPases (Vincent and Settleman, 1999). Recently, p120-catenin was shown to mediate RhoA inhibition via the recruitment of the p190A RhoGAP (Niessen and Yap, 2006; Wildenberg et al., 2006). This suggested that xARVCF-catenin might analogously associate with p190B, bridged or facilitated by Kazrin. Upon analysis of our yeast two-hybrid findings (alignment of limiting sequences from 22 independent

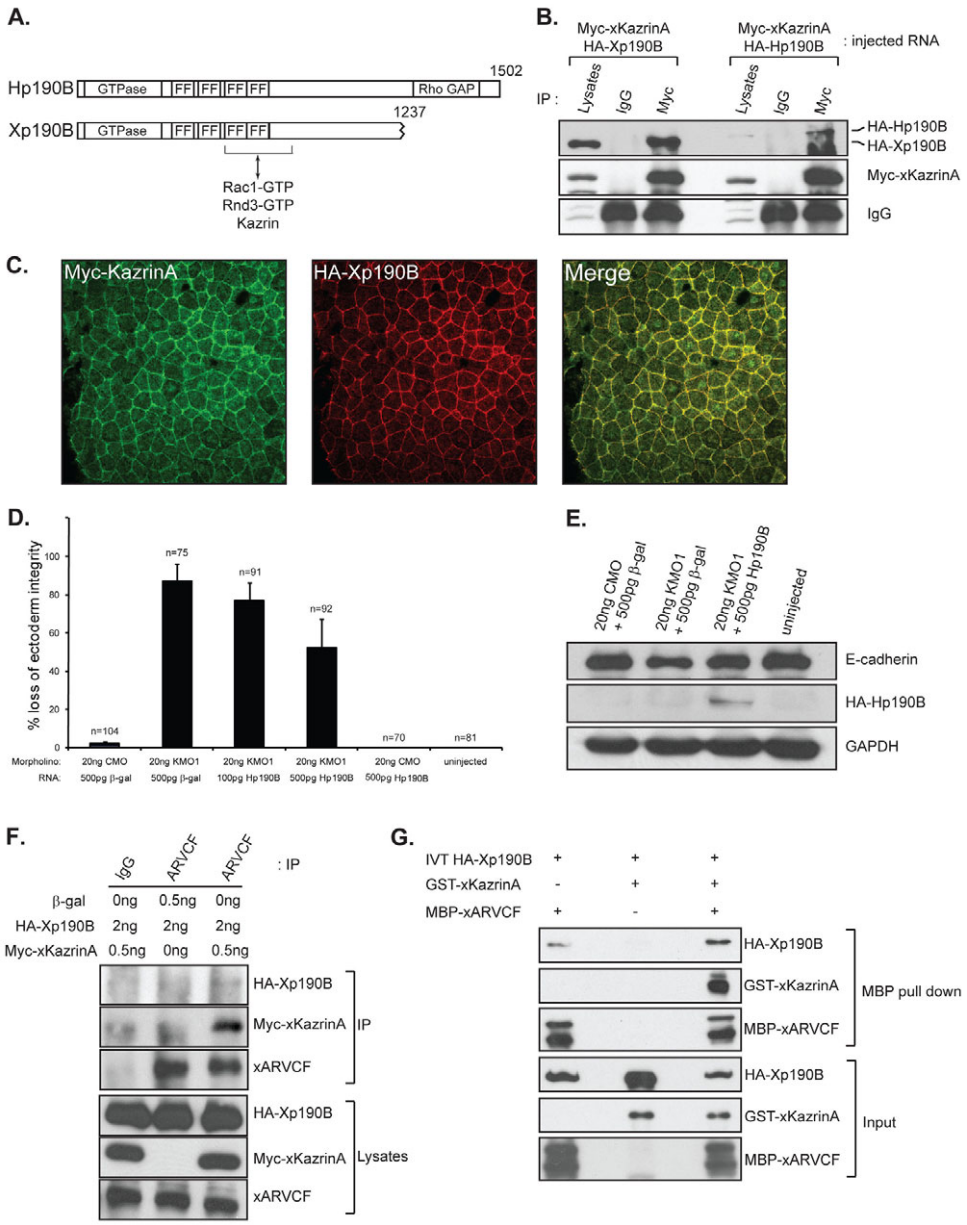

Fig. 9. Interaction of xKazrinA with Xp190B, and the role of xKazrinA in xARVCF–Xp190B RhoGAP association. (**A**) Comparison of human p190B (GeneBank ID # NM_001030055) and *Xenopus* p190B (BC084299.1). Protein domains were predicted using the SMART website (http://smart.embl-heidelberg.de/). The predicted binding region of Rnd proteins and Kazrin is shown. (**B**) In vivo binding of xKazrinA to human and *Xenopus* p190B. The indicated mRNAs were injected into one-cell embryos. Immunoprecipitates of Myc–xKazrinA were obtained from early gastrula (stage 10–11) extracts, followed by immunoblotting for p190Bs (HA antibody). (**C**) Colocalization of xKazrinA and Xp190B in blastula ectoderm. Blastula ectoderm (stage 9–10) coexpressing Myc–xKazrinA and HA–Xp190B was isolated, fixed and visualized by confocal fluorescent imaging for Myc and HA. (**D**) Partial rescue of ectoderm integrity, reduced following xKazrin depletion, upon expression of human p190B. Embryos were injected with the indicated amounts of morpholino and mRNA at the one-cell stage. Ectoderm integrity was evaluated at tailbud stage (stage 20–22) in three independent experiments. Error bars indicate standard error of the mean (s.e.m.). Numerical results are shown in supplementary material Table S3. (**E**) Ectopic p190B rescues xE-cadherin levels, reduced following xKazrin depletion. The indicated morpholinos and mRNAs were injected into one-cell embryos. Neurulation (stage 18) extracts were immunoblotted as indicated. (**F**) In vivo ternary complex formation of xARVCF–xKazrinA–Xp190B. Extracts from gastrula-stage embryos expressing the indicated proteins and endogenous xARVCF were precipitated for xARVCF. Co-precipitated xKazrinA and Xp190B were detected using antibodies directed against Myc and HA, respectively. (**G**) In vitro ternary protein complex of xARVCF–xKazrinA–Xp190B. In vitro transcribed and translated (IVT) Xp190B was incubated with bacterially purified GST–xKazrinA and MBP–xARVCF. Pull-down of xARVCF occurred using amylose–agarose beads, followed by immunoblotting as indicated.

clones), we deduce that xKazrinA binds to a region within or spanning the third to fourth FF domains of p190B (Fig. 9A; supplementary material Fig. S7) (Bedford and Leder, 1999). Interestingly, this portion of p190 RhoGAP also associates with activated Rac1 and Rnd3 (Rnd3 being a constitutively active RhoA antagonist), leaving open the possibility that Kazrin association with p190 RhoGAP might be competitive with that of Rac1 and Rnd3 (Fig. 9A) (Bustos et al., 2008; Wennerberg et al., 2003).

To further test the validity of the interaction of Kazrin with p190B, we undertook precipitations from embryo extracts and GST purified-component systems, using cDNA encoding human p190B, as well as the longest available (partial) cDNA encoding *Xenopus* p190B (79% sequence identity with human) (Fig. 9A; supplementary material Fig. S7). Following expression in vivo, both full-length human p190B and our partial Xp190B construct robustly coimmunoprecipitated with xKazrinA (Fig. 9B), and they colocalized to cell–cell borders (Fig. 9C). Finally, in a reductionist context suggesting their direct interaction, GST–xKazrin was co-precipitated with in vitro translated p190B (supplementary material Fig. S8).

Given their physical association, we asked whether the xKazrinA–p190B interaction might be functionally evident in vivo. For a read-out, we evaluated phenotypic rescue of ectodermal shedding, as described above for embryos depleted of xKazrin. Indeed, shedding phenotypes were partially but significantly rescued by titrated amounts of ectopic p190B (human full-length), and this occurred in a dose-dependent manner (Fig. 9D and supplementary material Table S3). These results support the concept that p190B and Kazrin are functionally coupled. Furthermore, the decrease in E-cadherin levels upon Kazrin depletion was restored by ectopic expression of human p190B RhoGAP (Fig. 9E), consistent with the possibility that lowered cadherin levels in Kazrin knockdown embryos might result from abnormal activation of RhoA.

To investigate whether xKazrin might facilitate p190B association with xARVCF, we asked whether Kazrin expression (versus not) had an impact on p190B association with xARVCF. As indicated in Fig. 9F (lane 3), a trace but reproducible amount of p190B was detected in complex with ARVCF only upon Kazrin coexpression. We next turned to in vitro pull-down assays to evaluate how p190B might associate with ARVCF (Fig. 9G). As expected on the basis of the precipitations from *Xenopus* extracts, in vitro translated Xp190B was pulled down with MBP–xARVCF in the presence of GST–xKazrinA (Fig. 9G, lane 3). This suggests that these three proteins form a ternary complex. Even in the absence of xKazrinA, Xp190B appeared to weakly bind xARVCF (Fig. 9G, lane 1). Thus, although requiring further study, it appears that Kazrin might recruit and/or enhance p190B association with ARVCF. In all cases, our data support the direct association and functional interaction of xKazrin with Xp190B RhoGAP.

In addition to xARVCF-catein, xKazrinA binds xδ-catenin and Xp0071-catenin

As mentioned, our xKazrin yeast two-hybrid screen suggested that, in addition to xARVCF-catenin, two related members of the p120 subfamily interact with xKazrinA, namely xδ-catenin and Xp0071-catenin (supplementary material Table S1). Pull-down validation tests were performed using purified GST–xKazrinA protein and in vitro translated xδ-catenin or Xp0071-catenin. Positive and negative controls, respectively, included xARVCF- and Xp120-catenin (Fig. 10). In agreement with our yeast two-hybrid assays, xARVCF-catenin, xδ-catenin and Xp0071-catenin bound xKazrinA, whereas Xp120-catenin did not. This suggests that the biochemical and presumably functional interactions of Kazrin involve some but not all p120 subfamily catenins.

Discussion

In this study we describe the identification of xKazrinA as a direct binding partner of xARVCF-catenin, a member of the p120-catenin subfamily. We additionally resolved the association of of xKazrinA with spectrin and p190B RhoGAP. Distinct from reported protein interactions of ARVCF or KazrinA at the adherens junction or desmosome, we find that KazrinA associates with spectrin. Specrin forms a cytoskeletal network that includes interactions with junctional constituents (Bennett and Healy, 2009; Kizhatil et al., 2007). Although requiring further study, Kazrin appears to enhance the association of ARVCF with p190B RhoGAP, with the reduction of RhoA activity by Kazrin being likely to occur via these same interactions (at least in part). Borrowing from independent studies (Gliem et al., 2010; Lamaze et al., 1996; Schmalzing et al., 1995; Sullivan et al., 1999), we postulate that such RhoA modulation is relevant to the organization of cortical actin and cadherin stability. On the basis of our rescue analyses, these biochemical and functional relationships appear to be relevant to effects observed following Kazrin depletion in *Xenopus* embryos, which included reduced ectodermal integrity (see Fig. 11). Finally, we find that some, but not all, p120 subfamily members (not p120-catenin) bind xKazrinA. Our results thus constitute an initial outline of the role of Kazrin in the context of catenins, RhoA and p190B RhoGAP.

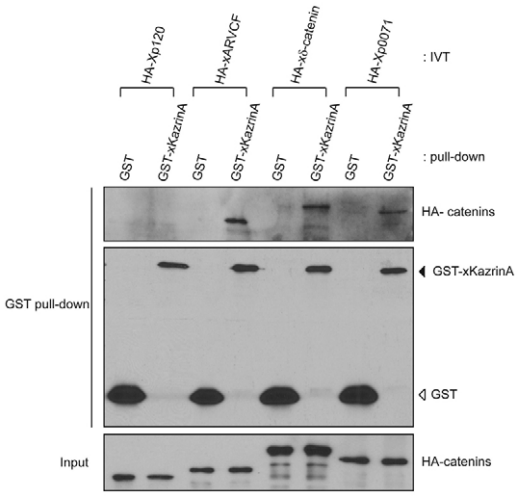

Fig. 10. In vitro binding of *Xenopus* p120 subfamily catenins to xKazrinA. (**A**) In vitro transcribed and translated (IVT) *Xenopus* p120 subfamily catenins (HA-tagged) were tested for association with GST–xKazrinA following GST pull-down and immunoblotting as indicated.

Kazrin isoforms and structure

Kazrin was originally identified as a cDNA (KIAA1026) expressed in human brain (Kikuno et al., 1999). In human keratinocytes, five Kazrin splice isoforms (KazrinA–Kazrin E) were then reported, along with their biochemical interactions and functional effects on keratinocyte differentiation, small GTPases and actin or microtubule networks (Groot et al., 2004; Nachat et al., 2009; Sevilla et al., 2008a). Adding to the functional complexity of Kazrin is KazrinF, recently reported to inhibit apoptosis through binding BAX (Bcl-2-associated X protein) and ARC (apoptosis repressor with caspase recruitment domain) in a human glioma cell line (Wang et al., 2009).

Our evaluation of KIAA1026 in particular showed that it lacks the NLS we characterized in other Kazrin isoforms, resulting in its exclusion from the nucleus. We propose that KIAA1026 be renamed KazrinK. Although the nuclear roles of all NLS-containing Kazrin isoforms are uncertain, both human KazrinE and human KazrinK associate with xARVCF (supplementary material Fig. S9B), possibly suggesting they have shared cytoplasmic and cytoskeletal functions.

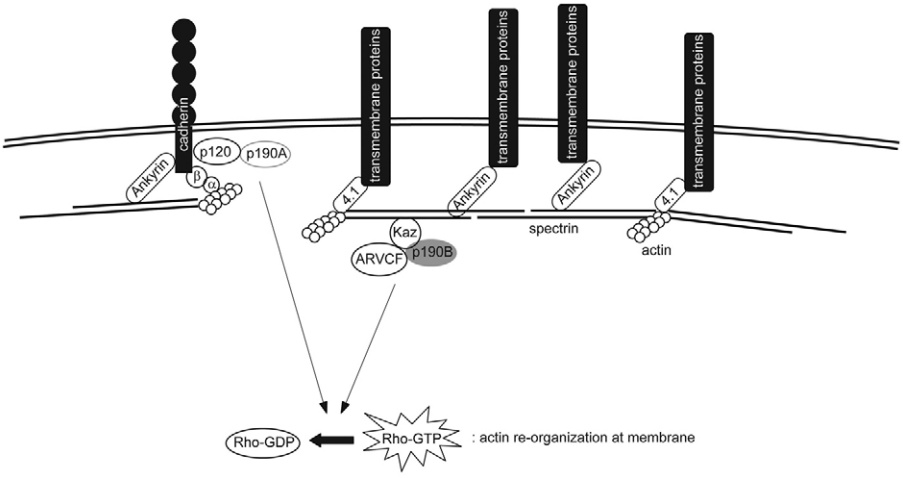

Fig. 11. Working model of xARVCF–xKazrinA complex localization and function at the plasma membrane. Kazrin (Kaz) facilitates formation of the trimeric ARVCF–p190B RhoGAP complex, which localizes to the plasma membrane via association of Kazrin with spectrin. This novel RhoGAP complex locally reduces RhoA activity at the plasma membrane and stabilizes the actin cytostructure, supporting cell–cell contacts. An interaction of p120-catenin with p190A RhoGAP at adherens junctions was previously reported (Wildenberg et al., 2006).

Structurally, xKazrin and its well-conserved vertebrate homologs are likely to represent a new protein group. All Kazrins examined share limited homology with the known coiled-coil regions as represented in Table 2. Secondary structural prediction of the coiled-coil region of Kazrin further indicated resemblances to the folding of spectrin repeats within α-spectrin (Pascual et al., 1997). Each of these proteins possesses extensive α-helical or coiled-coil structure engaging in homotypic or heterotypic protein–protein interactions (Burkhard et al., 2001). Indeed, we find that the heterotypic interactions between Kazrin and ARVCF requires the predicted coiled-coil domain of Kazrin (Fig. 3C,D). Although possible homotypic coiled-coil associations will require further study, we observed that xKazrinA constructs bearing different epitope tags co-precipitate (supplementary material Fig. S9A), and that human Kazrin isoforms co-associate in a human cell line (Nachat et al., 2009).

Protein partners of ARVCF-catenin

A number of proteins have been shown to directly bind ARVCF. These include cadherins, RhoA, Vav2, ERBIN, FRMPD2, ZO-1 and ZO-2 (Fang et al., 2004; Izawa et al., 2002; Kaufmann et al., 2000; Kausalya et al., 2004; Laura et al., 2002; Magie et al., 2002; Mariner et al., 2000; Noren et al., 2000; Paulson et al., 2000; Stenzel et al., 2009). The latter four each contain PDZ domains, which are thought to associate with PDZ binding motifs within the C-termini of ARVCF, δ-catenin and p0071. Our present study adds Kazrin as the newest binding partner of p120 subfamily members, excluding p120 itself. Kazrin seems to bind a relatively broad region of ARVCF (and probably other catenins), encompassing portions of the central Arm and C-terminal domains. In turn, the extended coiled-coil domain of Kazrin associates with ARVCF, such that the coiled-coil regions of each protein presumably interact. Because the Arm domain of ARVCF exhibits some homology with p120-catenin (55% identity and 74.4% similarity) (Sirotkin et al., 1997), it may prove interesting to resolve the basis of specificity among different p120 subfamily proteins. It will furthermore be relevant to test whether the larger ARVCF–Kazrin complex includes proteins known to bind via the PDZ binding motif within ARVCF, such as ERBIN (Laura et al., 2002), as this would provide further insight to the funcions of the complex.

Subcellular localization of the xARVCF–xKazrinA complex

In cornified epithelia and other primary and cultured cell types, Kazrin was visualized at plasma-membrane areas containing desmosomal and intermediate filament proteins, extradesmosomal areas enriched in cortical actin, and partially within cytoplasmic and nuclear compartments (Groot et al., 2004). In accordance with these results, and in common with ARVCF-, p120- and δ-catenin, we find that xKazrinA localizes to three subcellular regions: cell–cell borders, cytosol and the nucleus. Consistent with its nuclear localization, we resolved an NLS in the C-terminal region of xKazrinA (supplementary material Fig. S1). Interesting questions to address in future work include the nuclear function of Kazrin, possibly in a nuclear complex with ARVCF.

Initially, we addressed xARVCF and xKazrin localization to cell–cell borders, because although Kazrin is reported to bind periplakin and envoplakin at peripheral desmosomal or interdesmosomal regions in human keratinocytes (Groot et al., 2004), ARVCF is present at adherens junctions via binding cadherins (Kaufmann et al., 2000; Mariner et al., 2000; Paulson et al., 2000). Our present study indicates that the xARVCF–xKazrinA complex is not likely to be a core component of either adherens or desmosomal junctions. Instead, screening of xKazrinA resolved three (α2-, β1- and β2-) spectrin proteins as possible binding partners. Spectrins form a cytoskeletal network with actin filaments at the plasma membrane cortex, assisting in functions including plasma membrane and junctional strengthening, restriction of select proteins to plasma membrane subdomains, transduction of nerve action potentials, and contraction of heart cells (for a review, see Baines, 2009; Bennett and Healy, 2009). In this study, we found that the xARVCF–xKazrinA complex associates with xβ2-spectrin (Fig. 6), suggesting a novel interaction and localization of Kazrin and ARVCF-catenin (perhaps also δ-catenin and p0071). Previously, it was reported that the spectrin network associates with E-cadherin via ankyrin, contributing to lateral cell membrane integrity (Kizhatil et al., 2007). We, however, found neither C-cadherin nor p120 co-precipitating with β2-spectrin, despite significant homology within the cyto-domains of *Xenopus* E- and C-cadherin (80.5% identity). Possibly, cadherins such as C-cadherin form lesser interactions with the spectrin cytoskeleton in developmentally transitioning embryonic tissues.

Roles of the ARVCF–Kazrin complex

Earlier work predicted the involvement of Kazrin in clathrin-mediated endocytosis (Schmelzl and Geli, 2002), which is known to contribute to cadherin internalization and thereby to the modulation of junction function (Ivanov et al., 2004; Le et al., 1999; Xiao et al., 2005) (for reviews, see Bryant and Stow, 2004;

D'Souza-Schorey, 2005; Delva and Kowalczyk, 2009; Yap et al., 2007). Perhaps related are reports that p120 subfamily members protect cadherins from endocytosis and lysosomal degradation, and might also chaperone cadherins to the plasma membrane (Chen et al., 2003; Davis et al., 2003; Fang et al., 2004; Gu et al., 2009; Ireton et al., 2002; Xiao et al., 2003; Xiao et al., 2005) (for reviews, see Kowalczyk and Reynolds, 2004; Reynolds and Carnahan, 2004; Xiao et al., 2007). In desmosomal regions, Kazrin colocalizes with desmoglein3 (Fig. 5G–I), a desmosomal cadherin prone to accelerated endocytosis and degradation in the autoimmune disease pemphigus vulgaris (Calkins et al., 2006). We speculate that the role of Kazrin in endocytosis, or the role of the ARVCF–Kazrin complex, could be linked to reduced levels of cadherin and adhesion following Kazrin depletion.

If this were the case, one question would be how Kazrin, or the ARVCF–Kazrin complex, modulates cadherin endocytosis at the molecular level. Endocytosis requires cortical actin to be locally reorganized, with such changes involving the actions of small GTPases (for reviews, see Ellis and Mellor, 2000; Symons and Rusk, 2003). Multiple groups have reported Rho and Rac (and Cdc42) modulation by p120 subfamily catenins including ARVCF (Anastasiadis et al., 2000; Fang et al., 2004; Grosheva et al., 2001; Noren et al., 2000) (for a review, see Anastasiadis, 2007). Kazrin is similarly implicated in RhoA modulation (Sevilla et al., 2008a). Our results here point to negative xARVCF and xKazrin effects on RhoA activity (Fig. 8E), with the actin network becoming reorganized upon Kazrin depletion in vivo (Fig. 8F). Requiring future study, we speculate that the ARVCF–Kazrin complex modulates RhoA activity at cell contacts, having an impact on actin organization and thereby on cadherin stability and endocytosis. Interestingly, Charrasse and co-workers found that constitutively active RhoA induces M-cadherin endocytosis and degradation (following p120-catenin dissociation from M-cadherin) (Charrasse et al., 2006). Although there is a discrepancy between our results and theirs regarding p120 (Kazrin knockdown in *Xenopus* embryos decreased catenin protein levels, whereas RhoA activation in mouse myoblasts does not change endogenous p120 protein levels), both groups find that altered RhoA activity affects cadherin levels.

We identified p190B RhoGAP, ubiquitously expressed in mammals, as a novel binding partner of xKazrinA (Fig. 9 and supplementary material Table S1). Because p190A RhoGAP interacts with p120-catenin (Niessen and Yap, 2006; Wildenberg et al., 2006), and Xp190B with xARVCF (Fig. 9), p190 RhoGAP members might be core RhoA effectors of the p120 subfamily proteins (or vice versa). This view might also relate to an earlier report implicating p190 RhoGAP in RhoA inhibition upon cadherin engagement (Noren et al., 2003). Although we detected only weak endogenous association of Xp190B RhoGAP with xARVCF in vivo (Fig. 9F), their interaction might be regulated, conceivably in response to Rac1, Rnd proteins or tyrosine phophorylation by Src or Arg (Abl related gene) kinase (Brouns et al., 2001; Bustos et al., 2008; Hernandez et al., 2004; Wennerberg et al., 2003). Of note, overexpressed xARVCF partially rescues defective ectoderm integrity resulting from Kazrin depletion. Via the weak association of ARVCF with p190B, we speculate that properly titrated ARVCF overexpression might assist in recruiting p190B RhoGAP to cell–cell borders, thereby restoring a more physiological range of local RhoA activity.

Although Kazrin resides in both the nucleus and cytoplasm, as well as at cell–cell borders, the nuclear functions of Kazrin are uncertain. This and a prior study indicate that Kazrin affects cortical actin function via RhoA modulation (Sevilla et al., 2008a). Speculatively, Kazrin might also modulate nuclear actin, and thereby chromosome positioning and gene expression (Carmo-Fonseca, 2007; Chuang et al., 2006; Dundr et al., 2007). Additional nuclear functions might take place through association of Kazrin with coilin, a component of cajal bodies engaged in snRNP assembly and RNA splicing (Lim et al., 2006). Kazrin is further reported to associate with the meiotic apparatus of mouse unfertilized eggs (Gallicano et al., 2005), and with intermediate filaments (Groot et al., 2004), whereas a liprin-like isoform (KazrinE) associates with stable (acetylated) microtubules (Nachat et al., 2009). Given that ARVCF might bind Kazrin in the context of varied cell structures and compartments (Kaufmann et al., 2000; Mariner et al., 2000; Waibler et al., 2001), it will be especially interesting to discern whether either protein is relevant to the potential role of the other (or that of δ-catenin or p0071-catenin) in gene activity.

In all cases, our work here establishes xKazrin as a binding partner of xARVCF-catenin, with further related interactions occurring with p190B RhoGAP and spectrin. In keeping with a prior study (Sevilla et al., 2008b), xKazrin was shown to be essential in vivo, with our rescue analysis extending the functional interactions of Kazrin with xARVCF, cadherin and RhoA.

Materials and Methods

DNA constructs

For yeast two-hybrid screening, pGBT9/xARVCF-1ABC was generated via PCR and cloned into pGBT9 (Clontech). pMAL/xARVCF-1ABC was generated by cloning xARVCF-1ABC from pGBT9 into pMAL-C2x (New England Biolabs). pCS2/HA–xARVCF-1ABC was generated from pCS2/Myc–xARVCF-1ABC. pCS2/MT-xKazrinA was produced via PCR from *Xenopus* cDNA. pGEX/xKazrinA, pGEX/xKazrinA NT (amino acid residues 1–268), pGEX/xKazrinA CT (amino acid residues 263–409), pGEX/xKazrinA CC (amino acid residues 101–357) and pGEX/xKazrinA N were generated via PCR of cDNA. pCS2/MT-hKazrinK and pCS2/MT-hKazrinE were made by PCR of cDNA encoding human Kazrin. pCS2/MT-xKazrinA ΔN1 (amino acids 69–409), pCS2/MT-xKazrinA ΔN2 (amino acids 175–409), pCS2/MT-xKazrinA ΔC1 (amino acids 1–281), pCS2/MT-xKazrinA ΔC2 (amino acids 1–173) were made by excising DNA encoding pCS2/MT-xKazrinA with restriction enzymes and re-ligating to pCS2/Myc. pCS2/MT-xKazrinA ΔNLSC (amino acids 1–361) was generated by PCR into pCS2/Myc. pCS2/MT-xKazrinA NLSm was generated with the QuickChange kit (Stratagene). pMOM/HA was made by PCR of the Bcl-Xl MOM targeting sequence of Bcl-x [pEGFP-X-TMB (Bcl-x) was a gift of Christoph Borner (Albert-Ludwigs-University of Freiberg, Germany) (Kaufmann et al., 2003)], and cloned into pCS2/HA. pMOM/HA–xARVCF-1ABC, pMOM/HA–Xp120-1, pMOM/HA–xARVCF-Nmom (amino acids 1-296), pMOM/HA–xARVCF-Amom (amino acids 297–788), pMOM/HA–xARVCF-Cmom (amino acids 789-924), pMOM/HA–xARVCF-NAmom (amino acids 1-788), and pMOM/HA–xARVCF-ACmom (amino acids 297–924) were generated by PCR of the respective cDNAs and placed into pMOM/HA. cDNAs encoding *Xenopus* β2-spectrin and p190B (IMAGE #5571051 and # 6635626, respectively) were purchased from Open Biosystems (Thermo Fisher Scientific), and placed into pCS2/HA. cDNA encoding human p190B RhoGAP was a gift of Jeffrey M. Rosen (Baylor College of Medicine, Houston, TX) (Vargo-Gogola et al., 2006), and subcloned into pCS2/HA. pCS2/Myc–GFP–desmoglein1-tail was obtained as a gift of Michael W. Klymkowsky (University of Colorado). pCS2/HA–xδ-catenin construct was cloned previously (Gu et al., 2009). pCS2/HA–Xp0071 was a gift of Kris Vleminckx (unpublished; University of Ghent).

Antibodies and reagents

Anti-Myc (9E10) and anti *Xenopus* E-cadherin antibody (5D3), respectively developed by J. Michael Bishop and Barry M. Gumbiner, were obtained from the Developmental Studies Hybridoma Bank (NICHD and University of Iowa). Human Kazrin (LS7), C-cadherin, xARVCF, Xp120 and xβ-catenin antibodies are previously described (Fang et al., 2004; Nachat et al., 2009). Other antibodies were purchased from commercial sources (HA, Sigma H9658 and Santa Cruz Biotechnology SC805; β-actin, Sigma A2066; GAPDH, Santa Cruz Biotechnology SC-25778; RhoA, RhoB, RhoC, Millipore 05-822; desmoglein1, BD Transduction Laboratories 610273; plakoglobin, BD Transduction Laboratories 610253; human ARVCF, Abnova H00000421-M01; desmoplakin 1 and 2, BD Transduction Laboratories; β-catenin, BD Transduction Laboratories; and Myc for keratinocyte immunofluorescence, Bethyl Labs. Phosphatase Inhibitor Cocktail Set V was purchased from Calbiochem (EMD chemical), and included during the detection of in vivo p190B RhoGAP binding to xARVCF.

Yeast two-hybrid

Screening using full-length xARVCF-1ABC employed the *Saccharomyces cerevisiae* strain AH109 (Clontech), which was transformed with pGBT9/xARVCF-1ABC to generate the strain AH109/xARV. A *X. laevis* stage 18 cDNA library (Sparrow et al., 1998) in pGAD10 was transformed into AH109/xARV and 1×10^9 clones screened. Plasmids were isolated from colonies showing positive growth following replating, and were sequenced.

Screening using full-length xKazrinA employed an adult mouse brain cDNA library in collaboration with Hybrigenics ULTImate Y2H (Rain et al., 2009). We obtained 281 positive clones that were then sequenced and analyzed.

xKazrin RT-PCR primers and morpholino

Primers used for RT-PCR analysis of xKazrin were: F1, 5′-AGCTTCGGCGC-CAAGCCAAGG-3′ and R1, 5′-ACTCTGACAGCTTGCCGGTC-3′. We employed a previously characterized morpholino directed against xKazrin (KMO1) (xKazrin cDNA –4 to +21: 5′-GCTTGTTATCTTCCATCATCTTCAG-3′) (Sevilla et al., 2008b). A standard control morpholino (CMO) from Gene Tools LLC was used as a negative control (5′-CCTCTTACCTCAGTTACAATTTATA-3′).

GST pull-downs and blot overlay

For in vitro pull-down between xARVCF and xKazrinA, 1 mg of bacterially purified MBP–xARVCF or MBP–Xp120 were incubated with 1 mg of bacterially purified GST–xKazrinA in 1 ml of buffer (PBS, 1 mM EDTA, 0.1% NP-40, 100 ng/ml BSA) for 30 minutes with rocking at 4°C. Proteins were then precipitated using either glutathione-resin or amylose-resin, rinsed, and analyzed using SDS-PAGE and western blotting.

For in vitro MBP pull-down assays involving Xp190B, xARVCF and xKazrinA, 4 μg of DNA encoding pCS2/HA–Xp190B was in vitro transcribed and translated using the TNT SP6 High-Yield Wheat Germ Protein Expression System (Promega), following the manufacturer's protocol. Synthesized Xp190B protein was then incubated with 1 mg of GST–xKazrinA and/or MBP–xARVCF and pulled-down using amylose-resin.

For blot overlays, purified GST–xKazrinA or GST (250 ng each) was subject to SDS-PAGE and transferred to nitrocellulose. Resulting blots were incubated in PBS with 0.1% Tween-20 and 5% non-fat dry milk overnight at 4°C to facilitate refolding of the purified proteins, and then incubated for 1 hour at room temperature with 1 mg/ml purified MBP–xARVCF, MBP–Xp120 or MBP diluted in the same buffer. Associated MBP fusion proteins were detected using anti-MBP antibody.

Xenopus embryo manipulations, coimmunoprecipitations and cell–cell dissociation assays

Induction of female *X. laevis*, in vitro fertilization of eggs, and embryo injections were carried out using standard methods (Sive et al., 2000). Capped mRNAs for injection were generated using mMessage mMachine kits (Ambion). Embryos were incubated at 18°C to stage10 (early gastrula), lysed in embryo IP buffer (50 mM Tris-HCl pH 7.4, 1% Triton X-100, 150 mM NaCl, 1 mM EDTA, 1 mM PMSF, 1 mM Na_3VO_4, 1 mM NaF, and 1 mg/ml each of Aprotinin, leupeptin and pepstatin), centrifuged, and the supernatants divided for immunoprecipitation. Immune complexes were precipitated using Protein-A/G agarose beads (Santa Cruz Biotechnology), and subjected to western blotting.

For assay of cell–cell dissociation, naive ectoderm tissue fragments (animal caps) were isolated from late blastula embryos (stages 9–10), placed in 0.6× MMR solution with 2 mM EGTA and rotated at room temperature for 2–3 hours until control morpholino-injected animal caps were completely dissociated.

Cell culture

X. laevis A6 kidney epithelial cells were maintained in L15 media (Invitrogen) with 5% fetal bovine serum (Invitrogen), and kept at 22°C in a humidified incubator of normal atmosphere. Human MCF-7 breast cancer and HeLa cervical carcinoma cells were cultured in DMEM (Invitrogen), using standard mammalian cell culture conditions. A6 and MCF-7 cells were transfected using FuGene6 (Roche). Co-immunoprecipitations employed TX100 lysis buffer.

Normal human keratinocytes were isolated from neonatal foreskins and cultured in keratinocyte growth medium (KGM, Cambrex, East Rutherford, NJ), as described (Calkins et al., 2006). Keratinocytes at passage 4 or less were seeded into tissue culture vessels. Cells were switched into KGM medium containing 0.5 mM calcium 16–18 hours prior to fixation and immunostaining. Keratinocyte transient transfections were performed as described (DiColandrea et al., 2000).

Immunofluorescence

X. laevis A6 or human MCF-7 cells on coverslips were fixed 24–48 hours post-transfection in PBS with 3.7% formaldehyde for 5 minutes at room temperature. Samples were then permeabilized in PBS with 0.2% Triton X-100 for 10 minutes at room temperature, blocked for over 1 hour in antibody dilution buffer (PBS with 0.02% Triton X-100, 2% BSA and 2% normal donkey serum), and incubated for 1 hour each at room temperature with primary followed by secondary antibodies (donkey anti-rabbit-Cy3 or anti-mouse-FITC, Jackson Immunolabs). Samples were washed in blocking buffer three times and mounted on slides.

Keratinocytes on coverslips were fixed with 4% paraformaldehyde (PFA) and incubated with the indicated antibodies. Various Alexa-Fluors (Invitrogen, Carlsbad, CA) conjugated to species-specific secondary antibodies were used for dual-label immunofluorescence. Images were acquired using a Leica DMR-E fluorescence microscope, captured with a Hamamatsu Orca camera, and processed using Simple PCI software (Compix, Cranberry Township, PA). In limited cases, image brightness was adjusted using Adobe Photoshop software.

For *Xenopus* ectoderm confocal microscopy, in vitro transcribed mRNAs encoding Myc–xKazrinA and/or HA–xARVCF were injected into the animal pole of one-cell stage embryos. Vitelline membranes of late blastula embryos (stage 9) were manually removed, followed by a 2-hour fixation in MEMFA and methanol dehydration. Embryos were then serially re-hydrated with PBS-diluted methanol, incubated for 1 hour in blocking buffer (20% goat serum in PBST), incubated for 3 hours with primary antibody, washed for 1 hour with PBST, incubated for 3 hours with secondary antibodies and washed (3–4 times) with PBST. Blastula ectoderm tissue (animal caps) were isolated as described (Fang et al., 2004), and mounted on glass slides. Images obtained from an Olympus IX-70 inverted microscope were digitally captured using Olympus Fluoview FV500 software, and adjusted for brightness in select cases using Adobe Photoshop software.

For actin staining, naive ectoderm (animal caps) isolated at stage10 was fixed with 3.7% PFA and 0.25% glutaraldehyde in PBST for 30 minutes at room temperature. After rinsing with PBST, samples were incubated overnight at 4°C with Alexa Fluor 488–phalloidin (Molecular Probes/Invitrogen). Stained ectodermal tissues were washed with PBST, mounted and viewed under a confocal microscope.

In vitro Rho activity assay

In vitro Rho activity assays were performed as described (Gu et al., 2009). Briefly, *Xenopus* embryos injected with xARVCF and/or xKazrinA morpholinos were subject to lysis buffer (25 mM HEPES pH 7.5, 150 mM NaCl, 10 mg $MgCl_2$, 1% NP-40, 1 mM EDTA and 2% glycerol), and lysates incubated with recombinant GST–Rhotekin RBD (Rho binding domain) immobilized to glutathione-Sepharose 4B (GE Healthcare Life Science), followed by pull-down and subsequent SDS-PAGE and western blotting detection of active Rho.

We thank James C. Smith (University of Cambridge) for providing information regarding the *X. tropicalis* Kazrin cDNA sequence and morpholino design prior to publication (Sevilla et al., 2008b). We also thank Jeffrey M. Rosen, Michael W. Klymkowsky and Kris Vleminckx for sharing their DNA constructs. This work was supported by the National Institutes of Health (RO1-GM52112), a Texas ARP Grant and an Institutional Research Grant to PDM. KC was supported in part by a Hearst Foundation Student Research & Education Award, and TGV in part by a National Institutes of Health Training Grant (GM-5-T32-HD07325). RGB was supported by the Welch Foundation (G-0040). DNA sequencing and other core facilities were supported by a University of Texas MD Anderson Cancer Center NCI Core Grant (CA-16672). Deposited in PMC for release after 12 months.

Supplementary material available online at
http://jcs.biologists.org/cgi/content/full/123/23/4128/DC1

References

Aho, S., McLean, W. H., Li, K. and Uitto, J. (1998). cDNA cloning, mRNA expression, and chromosomal mapping of human and mouse periplakin genes. *Genomics* **48**, 242-247.

Akhtar, N. and Hotchin, N. A. (2001). RAC1 regulates adherens junctions through endocytosis of E-cadherin. *Mol. Biol. Cell* **12**, 847-862.

Anastasiadis, P. Z. (2007). p120-ctn: A nexus for contextual signaling via Rho GTPases. *Biochim. Biophys. Acta* **1773**, 34-46.

Anastasiadis, P. Z., Moon, S. Y., Thoreson, M. A., Mariner, D. J., Crawford, H. C., Zheng, Y. and Reynolds, A. B. (2000). Inhibition of RhoA by p120 catenin. *Nat. Cell Biol.* **2**, 637-644.

Aono, S., Nakagawa, S., Reynolds, A. B. and Takeichi, M. (1999). p120(ctn) acts as an inhibitory regulator of cadherin function in colon carcinoma cells. *J. Cell Biol.* **145**, 551-562.

Baines, A. J. (2009). Evolution of spectrin function in cytoskeletal and membrane networks. *Biochem. Soc. Trans.* **37**, 796-803.

Baines, A. J., Bignone, P. A., King, M. D., Maggs, A. M., Bennett, P. M., Pinder, J. C. and Phillips, G. W. (2009). The CKK domain (DUF1781) binds microtubules and defines the CAMSAP/ssp4 family of animal proteins. *Mol. Biol. Evol.* **26**, 2005-2014.

Baki, L., Marambaud, P., Efthimiopoulos, S., Georgakopoulos, A., Wen, P., Cui, W., Shioi, J., Koo, E., Ozawa, M., Friedrich, V. L., Jr et al. (2001). Presenilin-1 binds cytoplasmic epithelial cadherin, inhibits cadherin/p120 association, and regulates stability and function of the cadherin/catenin adhesion complex. *Proc. Natl. Acad. Sci. USA* **98**, 2381-2386.

Bedford, M. T. and Leder, P. (1999). The FF domain: a novel motif that often accompanies WW domains. *Trends Biochem. Sci.* **24**, 264-265.

Bennett, V. and Healy, J. (2009). Membrane domains based on ankyrin and spectrin associated with cell-cell interactions. *Cold Spring Harbor Perspect. Biol.* **1**, a003012.

Borrmann, C. M., Grund, C., Kuhn, C., Hofmann, I., Pieperhoff, S. and Franke, W. W. (2006). The area composita of adhering junctions connecting heart muscle cells of vertebrates. II. Colocalizations of desmosomal and fascia adhaerens molecules in the intercalated disk. *Eur. J. Cell Biol.* **85**, 469-485.

Brouns, M. R., Matheson, S. F. and Settleman, J. (2001). p190 RhoGAP is the principal Src substrate in brain and regulates axon outgrowth, guidance and fasciculation. *Nat. Cell Biol.* **3**, 361-367.

Bryant, D. M. and Stow, J. L. (2004). The ins and outs of E-cadherin trafficking. *Trends Cell Biol.* **14**, 427-434.

Burkhard, P., Stetefeld, J. and Strelkov, S. V. (2001). Coiled coils: a highly versatile protein folding motif. *Trends Cell. Biol.* **11**, 82-88.

Bustos, R. I., Forget, M. A., Settleman, J. E. and Hansen, S. H. (2008). Coordination of Rho and Rac GTPase function via p190B RhoGAP. *Curr. Biol.* **18**, 1606-1611.

Cadigan, K. M. and Peifer, M. (2009). Wnt signaling from development to disease: insights from model systems. *Cold Spring Harbor Perspect. Biol.* **1**, a002881.

Calkins, C. C., Setzer, S. V., Jennings, J. M., Summers, S., Tsunoda, K., Amagai, M. and Kowalczyk, A. P. (2006). Desmoglein endocytosis and desmosome disassembly are coordinated responses to pemphigus autoantibodies. *J. Biol. Chem.* **281**, 7623-7634.

Carmo-Fonseca, M. (2007). How genes find their way inside the cell nucleus. *J. Cell Biol.* **179**, 1093-1094.

Charrasse, S., Comunale, F., Grumbach, Y., Poulat, F., Blangy, A. and Gauthier-Rouviere, C. (2006). RhoA GTPase regulates M-cadherin activity and myoblast fusion. *Mol. Biol. Cell* **17**, 749-759.

Chen, X., Kojima, S., Borisy, G. G. and Green, K. J. (2003). p120 catenin associates with kinesin and facilitates the transport of cadherin-catenin complexes to intercellular junctions. *J. Cell Biol.* **163**, 547-557.

Choi, H. J. and Weis, W. I. (2005). Structure of the armadillo repeat domain of plakophilin 1. *J. Mol. Biol.* **346**, 367-376.

Chuang, C. H., Carpenter, A. E., Fuchsova, B., Johnson, T., de Lanerolle, P. and Belmont, A. S. (2006). Long-range directional movement of an interphase chromosome site. *Curr. Biol.* **16**, 825-831.

Cokol, M., Nair, R. and Rost, B. (2000). Finding nuclear localization signals. *EMBO Rep.* **1**, 411-415.

Daniel, J. M. (2007). Dancing in and out of the nucleus: p120(ctn) and the transcription factor Kaiso. *Biochim. Biophys. Acta* **1773**, 59-68.

Daniel, J. M. and Reynolds, A. B. (1999). The catenin p120(ctn) interacts with Kaiso, a novel BTB/POZ domain zinc finger transcription factor. *Mol. Cell. Biol.* **19**, 3614-3623.

Davis, M. A., Ireton, R. C. and Reynolds, A. B. (2003). A core function for p120-catenin in cadherin turnover. *J. Cell Biol.* **163**, 525-534.

Delva, E. and Kowalczyk, A. P. (2009). Regulation of cadherin trafficking. *Traffic* **10**, 259-267.

DiColandrea, T., Karashima, T., Maatta, A. and Watt, F. M. (2000). Subcellular distribution of envoplakin and periplakin: insights into their role as precursors of the epidermal cornified envelope. *J. Cell Biol.* **151**, 573-586.

D'Souza-Schorey, C. (2005). Disassembling adherens junctions: breaking up is hard to do. *Trends Cell Biol.* **15**, 19-26.

Dundr, M., Ospina, J. K., Sung, M. H., John, S., Upender, M., Ried, T., Hager, G. L. and Matera, A. G. (2007). Actin-dependent intranuclear repositioning of an active gene locus in vivo. *J. Cell Biol.* **179**, 1095-1103.

Ellis, S. and Mellor, H. (2000). Regulation of endocytic traffic by rho family GTPases. *Trends Cell Biol.* **10**, 85-88.

Fang, X., Ji, H., Kim, S. W., Park, J. I., Vaught, T. G., Anastasiadis, P. Z., Ciesiolka, M. and McCrea, P. D. (2004). Vertebrate development requires ARVCF and p120 catenins and their interplay with RhoA and Rac. *J. Cell Biol.* **165**, 87-98.

Fujita, Y., Krause, G., Scheffner, M., Zechner, D., Leddy, H. E., Behrens, J., Sommer, T. and Birchmeier, W. (2002). Hakai, a c-Cbl-like protein, ubiquitinates and induces endocytosis of the E-cadherin complex. *Nat. Cell Biol.* **4**, 222-231.

Gallicano, G. I., Foshay, K., Pengetnze, Y. and Zhou, X. (2005). Dynamics and unexpected localization of the plakin binding protein, kazrin, in mouse eggs and early embryos. *Dev. Dyn.* **234**, 201-214.

Giebelhaus, D. H., Zelus, B. D., Henchman, S. K. and Moon, R. T. (1987). Changes in the expression of alpha-fodrin during embryonic development of *Xenopus laevis*. *J. Cell Biol.* **105**, 843-853.

Gliem, M., Heupel, W. M., Spindler, V., Harms, G. S. and Waschke, J. (2010). Actin reorganization contributes to loss of cell adhesion in pemphigus vulgaris. *Am. J. Physiol. Cell Physiol.* **299**, C606-C613.

Groot, K. R., Sevilla, L. M., Nishi, K., DiColandrea, T. and Watt, F. M. (2004). Kazrin, a novel periplakin-interacting protein associated with desmosomes and the keratinocyte plasma membrane. *J. Cell Biol.* **166**, 653-659.

Grosheva, I., Shtutman, M., Elbaum, M. and Bershadsky, A. D. (2001). p120 catenin affects cell motility via modulation of activity of Rho-family GTPases: a link between cell-cell contact formation and regulation of cell locomotion. *J. Cell Sci.* **114**, 695-707.

Gu, D., Sater, A. K., Ji, H., Cho, K., Clark, M., Stratton, S. A., Barton, M. C., Lu, Q. and McCrea, P. D. (2009). *Xenopus* δ-catenin is essential in early embryogenesis and is functionally linked to cadherins and small GTPases. *J. Cell Sci.* **122**, 4049-4061.

Hall, R. A. (2004). Studying protein-protein interactions via blot overlay or far western blot. *Methods Mol. Biol.* **261**, 167-174.

Heasman, J., Ginsberg, D., Geiger, B., Goldstone, K., Pratt, T., Yoshida-Noro, C. and Wylie, C. (1994). A functional test for maternally inherited cadherin in *Xenopus* shows its importance in cell adhesion at the blastula stage. *Development* **120**, 49-57.

Hernandez, S. E., Settleman, J. and Koleske, A. J. (2004). Adhesion-dependent regulation of p190RhoGAP in the developing brain by the Abl-related gene tyrosine kinase. *Curr. Biol.* **14**, 691-696.

Hong, J. Y., Park, J., Cho, K., Gu, D., Ji, H., Artandi, S. E. and McCrea, P. D. (2010). Shared molecular mechanisms regulate multiple catenin proteins: canonical Wnt signals and components modulate p120-catenin isoform-1 and additional p120 subfamily members *J. Cell Sci.* in press.

Huber, A. H., Nelson, W. J. and Weis, W. I. (1997). Three-dimensional structure of the armadillo repeat region of beta-catenin. *Cell* **90**, 871-882.

Iioka, H., Doerner, S. K. and Tamai, K. (2009). Kaiso is a bimodal modulator for Wnt/beta-catenin signaling. *FEBS Lett.* **583**, 627-632.

Ireton, R. C., Davis, M. A., van Hengel, J., Mariner, D. J., Barnes, K., Thoreson, M. A., Anastasiadis, P. Z., Matrisian, L., Bundy, L. M., Sealy, L. et al. (2002). A novel role for p120 catenin in E-cadherin function. *J. Cell Biol.* **159**, 465-476.

Ivanov, A. I., Nusrat, A. and Parkos, C. A. (2004). Endocytosis of epithelial apical junctional proteins by a clathrin-mediated pathway into a unique storage compartment. *Mol. Biol. Cell* **15**, 176-188.

Izawa, I., Nishizawa, M., Tomono, Y., Ohtakara, K., Takahashi, T. and Inagaki, M. (2002). ERBIN associates with p0071, an armadillo protein, at cell-cell junctions of epithelial cells. *Genes Cells* **7**, 475-485.

Izumi, G., Sakisaka, T., Baba, T., Tanaka, S., Morimoto, K. and Takai, Y. (2004). Endocytosis of E-cadherin regulated by Rac and Cdc42 small G proteins through IQGAP1 and actin filaments. *J. Cell Biol.* **166**, 237-248.

Johnson, K. J. and Boekelheide, K. (2002). Dynamic testicular adhesion junctions are immunologically unique. I. Localization of p120 catenin in rat testis. *Biol. Reprod.* **66**, 983-991.

Jones, D. T., Tress, M., Bryson, K. and Hadley, C. (1999). Successful recognition of protein folds using threading methods biased by sequence similarity and predicted secondary structure. *Proteins* **3**, 104-111.

Kanno, M., Aoyama, Y., Isa, Y., Yamamoto, Y. and Kitajima, Y. (2008a). P120 catenin is associated with desmogleins when desmosomes are assembled in high-Ca^{2+} medium but not when disassembled in low-Ca^{2+} medium in DJM-1 cells. *J. Dermatol.* **35**, 317-324.

Kanno, M., Isa, Y., Aoyama, Y., Yamamoto, Y., Nagai, M., Ozawa, M. and Kitajima, Y. (2008b). P120-catenin is a novel desmoglein 3 interacting partner: identification of the p120-catenin association site of desmoglein 3. *Exp. Cell Res.* **314**, 1683-1692.

Kaufmann, T., Schlipf, S., Sanz, J., Neubert, K., Stein, R. and Borner, C. (2003). Characterization of the signal that directs Bcl-x(L), but not Bcl-2, to the mitochondrial outer membrane. *J. Cell Biol.* **160**, 53-64.

Kaufmann, U., Zuppinger, C., Waibler, Z., Rudiger, M., Urbich, C., Martin, B., Jockusch, B. M., Eppenberger, H. and Starzinski-Powitz, A. (2000). The armadillo repeat region targets ARVCF to cadherin-based cellular junctions. *J. Cell Sci.* **113**, 4121-4135.

Kausalya, P. J., Phua, D. C. and Hunziker, W. (2004). Association of ARVCF with zonula occludens (ZO)-1 and ZO-2: binding to PDZ-domain proteins and cell-cell adhesion regulate plasma membrane and nuclear localization of ARVCF. *Mol. Biol. Cell* **15**, 5503-5515.

Keon, B. H., Schafer, S., Kuhn, C., Grund, C. and Franke, W. W. (1996). Symplekin, a novel type of tight junction plaque protein. *J. Cell Biol.* **134**, 1003-1018.

Kikuno, R., Nagase, T., Ishikawa, K., Hirosawa, M., Miyajima, N., Tanaka, A., Kotani, H., Nomura, N. and Ohara, O. (1999). Prediction of the coding sequences of unidentified human genes. XIV. The complete sequences of 100 new cDNA clones from brain which code for large proteins in vitro. *DNA Res.* **6**, 197-205.

Kim, S. W., Fang, X., Ji, H., Paulson, A. F., Daniel, J. M., Ciesiolka, M., van Roy, F. and McCrea, P. D. (2002). Isolation and characterization of XKaiso, a transcriptional repressor that associates with the catenin Xp120(ctn) in *Xenopus laevis*. *J. Biol. Chem.* **277**, 8202-8208.

Kim, S. W., Park, J. I., Spring, C. M., Sater, A. K., Ji, H., Otchere, A. A., Daniel, J. M. and McCrea, P. D. (2004). Non-canonical Wnt signals are modulated by the Kaiso transcriptional repressor and p120-catenin. *Nat. Cell Biol.* **6**, 1212-1220.

Kizhatil, K., Davis, J. Q., Davis, L., Hoffman, J., Hogan, B. L. and Bennett, V. (2007). Ankyrin-G is a molecular partner of E-cadherin in epithelial cells and early embryos. *J. Biol. Chem.* **282**, 26552-26561.

Klein, S. L., Strausberg, R. L., Wagner, L., Pontius, J., Clifton, S. W. and Richardson, P. (2002). Genetic and genomic tools for *Xenopus* research: The NIH *Xenopus* initiative. *Dev. Dyn.* **225**, 384-391.

Kowalczyk, A. P. and Reynolds, A. B. (2004). Protecting your tail: regulation of cadherin degradation by p120-catenin. *Curr. Opin. Cell Biol.* **16**, 522-527.

Lamaze, C., Chuang, T. H., Terlecky, L. J., Bokoch, G. M. and Schmid, S. L. (1996). Regulation of receptor-mediated endocytosis by Rho and Rac. *Nature* **382**, 177-179.

Laura, R. P., Witt, A. S., Held, H. A., Gerstner, R., Deshayes, K., Koehler, M. F., Kosik, K. S., Sidhu, S. S. and Lasky, L. A. (2002). The Erbin PDZ domain binds with high affinity and specificity to the carboxyl termini of delta-catenin and ARVCF. *J. Biol. Chem.* **277**, 12906-12914.

Le T. L., Yap, A. S. and Stow, J. L. (1999). Recycling of E-cadherin: a potential mechanism for regulating cadherin dynamics. *J. Cell Biol.* **146**, 219-232.

Lee, C. H. and Gumbiner, B. M. (1995). Disruption of gastrulation movements in *Xenopus* by a dominant-negative mutant for C-cadherin. *Dev. Biol.* **171**, 363-373.

Leung, S. M., Rojas, R., Maples, C., Flynn, C., Ruiz, W. G., Jou, T. S. and Apodaca, G. (1999). Modulation of endocytic traffic in polarized Madin-Darby canine kidney cells by the small GTPase RhoA. *Mol. Biol. Cell* **10**, 4369-4384.

Lim, J., Hao, T., Shaw, C., Patel, A. J., Szabo, G., Rual, J. F., Fisk, C. J., Li, N., Smolyar, A., Hill, D. E. et al. (2006). A protein-protein interaction network for human inherited ataxias and disorders of Purkinje cell degeneration. *Cell* **125**, 801-814.

Lupas, A., Van Dyke, M. and Stock, J. (1991). Predicting coiled coils from protein sequences. *Science* **252**, 1162-1164.
Macia, E., Ehrlich, M., Massol, R., Boucrot, E., Brunner, C. and Kirchhausen, T. (2006). Dynasore, a cell-permeable inhibitor of dynamin. *Dev. Cell* **10**, 839-850.
Magie, C. R., Pinto-Santini, D. and Parkhurst, S. M. (2002). Rho1 interacts with p120ctn and alpha-catenin, and regulates cadherin-based adherens junction components in Drosophila. *Development* **129**, 3771-3782.
Marambaud, P., Shioi, J., Serban, G., Georgakopoulos, A., Sarner, S., Nagy, V., Baki, L., Wen, P., Efthimiopoulos, S., Shao, Z. et al. (2002). A presenilin-1/gamma-secretase cleavage releases the E-cadherin intracellular domain and regulates disassembly of adherens junctions. *EMBO J.* **21**, 1948-1956.
Mariner, D. J., Wang, J. and Reynolds, A. B. (2000). ARVCF localizes to the nucleus and adherens junction and is mutually exclusive with p120(ctn) in E-cadherin complexes. *J. Cell Sci.* **113**, 1481-1490.
McCrea, P. D., Gu, D. and Balda, M. S. (2009). Junctional music that the nucleus hears: cell-cell contact signaling and the modulation of gene activity. *Cold Spring Harbor Perspect. Biol.* **1**, a002923.
Nachat, R., Cipolat, S., Sevilla, L. M., Chhatriwala, M., Groot, K. R. and Watt, F. M. (2009). KazrinE is a desmosome-associated liprin that colocalises with acetylated microtubules. *J. Cell Sci.* **122**, 4035-4041.
Niessen, C. M. and Yap, A. S. (2006). Another job for the talented p120-catenin. *Cell* **127**, 875-877.
Noren, N. K., Liu, B. P., Burridge, K. and Kreft, B. (2000). p120 catenin regulates the actin cytoskeleton via Rho family GTPases. *J. Cell Biol.* **150**, 567-580.
Noren, N. K., Arthur, W. T. and Burridge, K. (2003). Cadherin engagement inhibits RhoA via p190RhoGAP. *J. Biol. Chem.* **278**, 13615-13618.
Ohkubo, T. and Ozawa, M. (1999). p120(ctn) binds to the membrane-proximal region of the E-cadherin cytoplasmic domain and is involved in modulation of adhesion activity. *J. Biol. Chem.* **274**, 21409-21415.
Ozawa, M. and Kemler, R. (1998). The membrane-proximal region of the E-cadherin cytoplasmic domain prevents dimerization and negatively regulates adhesion activity. *J. Cell Biol.* **142**, 1605-1613.
Ozawa, M., Baribault, H. and Kemler, R. (1989). The cytoplasmic domain of the cell adhesion molecule uvomorulin associates with three independent proteins structurally related in different species. *EMBO J.* **8**, 1711-1717.
Papkoff, J. (1997). Regulation of complexed and free catenin pools by distinct mechanisms. Differential effects of Wnt-1 and v-Src. *J. Biol. Chem.* **272**, 4536-4543.
Park, J. I., Kim, S. W., Lyons, J. P., Ji, H., Nguyen, T. T., Cho, K., Barton, M. C., Deroo, T., Vleminckx, K., Moon, R. T. et al. (2005). Kaiso/p120-catenin and TCF/beta-catenin complexes coordinately regulate canonical Wnt gene targets. *Dev. Cell* **8**, 843-854.
Park, J. I., Ji, H., Jun, S., Gu, D., Hikasa, H., Li, L., Sokol, S. Y. and McCrea, P. D. (2006). Frodo links Dishevelled to the p120-catenin/Kaiso pathway: distinct catenin subfamilies promote Wnt signals. *Dev. Cell* **11**, 683-695.
Pascual, J., Pfuhl, M., Walther, D., Saraste, M. and Nilges, M. (1997). Solution structure of the spectrin repeat: a left-handed antiparallel triple-helical coiled-coil. *J. Mol. Biol.* **273**, 740-751.
Paterson, H. F., Self, A. J., Garrett, M. D., Just, I., Aktories, K. and Hall, A. (1990). Microinjection of recombinant p21rho induces rapid changes in cell morphology. *J. Cell Biol.* **111**, 1001-1007.
Paulson, A. F., Mooney, E., Fang, X., Ji, H. and McCrea, P. D. (2000). Xarvcf, *Xenopus* member of the p120 catenin subfamily associating with cadherin juxtamembrane region. *J. Biol. Chem.* **275**, 30124-30131.
Peifer, M., Berg, S. and Reynolds, A. B. (1994). A repeating amino acid motif shared by proteins with diverse cellular roles. *Cell* **76**, 789-791.
Rain, J. C., Cribier, A., Gerard, A., Emiliani, S. and Benarous, R. (2009). Yeast two-hybrid detection of integrase-host factor interactions. *Methods* **47**, 291-297.
Reynolds, A. B. and Carnahan, R. H. (2004). Regulation of cadherin stability and turnover by p120ctn: implications in disease and cancer. *Semin. Cell Dev. Biol.* **15**, 657-663.
Ruzov, A., Hackett, J. A., Prokhortchouk, A., Reddington, J. P., Madej, M. J., Dunican, D. S., Prokhortchouk, E., Pennings, S. and Meehan, R. R. (2009a). The interaction of xKaiso with xTcf3: a revised model for integration of epigenetic and Wnt signalling pathways. *Development* **136**, 723-727.
Ruzov, A., Savitskaya, E., Hackett, J. A., Reddington, J. P., Prokhortchouk, A., Madej, M. J., Chekanov, N., Li, M., Dunican, D. S., Prokhortchouk, E. et al. (2009b). The non-methylated DNA-binding function of Kaiso is not required in early *Xenopus laevis* development. *Development* **136**, 729-738.
Schmalzing, G., Richter, H. P., Hansen, A., Schwarz, W., Just, I. and Aktories, K. (1995). Involvement of the GTP binding protein Rho in constitutive endocytosis in *Xenopus laevis* oocytes. *J. Cell Biol.* **130**, 1319-1332.
Schmelzl, B. and Geli, M. I. (2002). An efficient genetic screen in mammalian cultured cells. *EMBO Rep.* **3**, 682-687.
Sevilla, L. M., Nachat, R., Groot, K. R. and Watt, F. M. (2008a). Kazrin regulates keratinocyte cytoskeletal networks, intercellular junctions and differentiation. *J. Cell Sci.* **121**, 3561-3569.
Sevilla, L. M., Rana, A. A., Watt, F. M. and Smith, J. C. (2008b). KazrinA is required for axial elongation and epidermal integrity in *Xenopus tropicalis*. *Dev. Dyn.* **237**, 1718-1725.
Sirotkin, H., O'Donnell, H., DasGupta, R., Halford, S., St Jore, B., Puech, A., Parimoo, S., Morrow, B., Skoultchi, A., Weissman, S. M. et al. (1997). Identification of a new human catenin gene family member (ARVCF) from the region deleted in velo-cardio-facial syndrome. *Genomics* **41**, 75-83.
Sive, H. L., Grainger, R. M. and Harland, R. M. (2000). *Early Development of Xenopus laevis: a Laboratory Manual*. Cold Spring Harbor, New York: Cold Spring Harbor Laboratory Press.
Sparrow, D. B., Kotecha, S., Towers, N. and Mohun, T. J. (1998). *Xenopus* eHAND: a marker for the developing cardiovascular system of the embryo that is regulated by bone morphogenetic proteins. *Mech. Dev.* **71**, 151-163.
Spring, C. M., Kelly, K. F., O'Kelly, I., Graham, M., Crawford, H. C. and Daniel, J. M. (2005). The catenin p120ctn inhibits Kaiso-mediated transcriptional repression of the beta-catenin/TCF target gene matrilysin. *Exp. Cell Res.* **305**, 253-265.
Stenzel, N., Fetzer, C. P., Heumann, R. and Erdmann, K. S. (2009). PDZ-domain-directed basolateral targeting of the peripheral membrane protein FRMPD2 in epithelial cells. *J. Cell Sci.* **122**, 3374-3384.
Sullivan, R., Price, L. S. and Koffer, A. (1999). Rho controls cortical F-actin disassembly in addition to, but independently of, secretion in mast cells. *J. Biol. Chem.* **274**, 38140-38146.
Symons, M. and Rusk, N. (2003). Control of vesicular trafficking by Rho GTPases. *Curr. Biol.* **13**, R409-R418.
Thoreson, M. A., Anastasiadis, P. Z., Daniel, J. M., Ireton, R. C., Wheelock, M. J., Johnson, K. R., Hummingbird, D. K. and Reynolds, A. B. (2000). Selective uncoupling of p120(ctn) from E-cadherin disrupts strong adhesion. *J. Cell Biol.* **148**, 189-202.
Turner, A. P., Brown, D., Heasman, J., Cook, G. M., Evans, J., Vickers, L. and Wylie, C. C. (1992). Involvement of a neutral glycolipid in differential cell adhesion in the *Xenopus* blastula. *EMBO J.* **11**, 3845-3855.
Vargo-Gogola, T., Heckman, B. M., Gunther, E. J., Chodosh, L. A. and Rosen, J. M. (2006). P190-B Rho GTPase-activating protein overexpression disrupts ductal morphogenesis and induces hyperplastic lesions in the developing mammary gland. *Mol. Endocrinol.* **20**, 1391-1405.
Vincent, S. and Settleman, J. (1999). Inhibition of RhoGAP activity is sufficient for the induction of Rho-mediated actin reorganization. *Eur. J. Cell Biol.* **78**, 539-548.
Waibler, Z., Schafer, A. and Starzinski-Powitz, A. (2001). mARVCF cellular localisation and binding to cadherins is influenced by the cellular context but not by alternative splicing. *J. Cell Sci.* **114**, 3873-3884.
Wang, Q., Liu, M., Li, X., Chen, L. and Tang, H. (2009). Kazrin F is involved in apoptosis and interacts with BAX and ARC. *Acta Biochim. Biophys. Sin. (Shanghai)* **41**, 763-772.
Wennerberg, K., Forget, M. A., Ellerbroek, S. M., Arthur, W. T., Burridge, K., Settleman, J., Der, C. J. and Hansen, S. H. (2003). Rnd proteins function as RhoA antagonists by activating p190 RhoGAP. *Curr. Biol.* **13**, 1106-1115.
Wildenberg, G. A., Dohn, M. R., Carnahan, R. H., Davis, M. A., Lobdell, N. A., Settleman, J. and Reynolds, A. B. (2006). p120-catenin and p190RhoGAP regulate cell-cell adhesion by coordinating antagonism between Rac and Rho. *Cell* **127**, 1027-1039.
Xiao, K., Allison, D. F., Buckley, K. M., Kottke, M. D., Vincent, P. A., Faundez, V. and Kowalczyk, A. P. (2003). Cellular levels of p120 catenin function as a set point for cadherin expression levels in microvascular endothelial cells. *J. Cell Biol.* **163**, 535-545.
Xiao, K., Garner, J., Buckley, K. M., Vincent, P. A., Chiasson, C. M., Dejana, E., Faundez, V. and Kowalczyk, A. P. (2005). p120-Catenin regulates clathrin-dependent endocytosis of VE-cadherin. *Mol. Biol. Cell* **16**, 5141-5151.
Xiao, K., Oas, R. G., Chiasson, C. M. and Kowalczyk, A. P. (2007). Role of p120-catenin in cadherin trafficking. *Biochim. Biophys. Acta* **1773**, 8-16.
Yamamoto, M., Yoshimura, K., Kitada, M., Nakahara, J., Seiwa, C., Ueki, T., Shimoda, Y., Ishige, A., Watanabe, K. and Asou, H. (2009). A new monoclonal antibody, A3B10, specific for astrocyte-lineage cells recognizes calmodulin-regulated spectrin-associated protein 1 (Camsap1). *J. Neurosci. Res.* **87**, 503-513.
Yap, A. S., Niessen, C. M. and Gumbiner, B. M. (1998). The juxtamembrane region of the cadherin cytoplasmic tail supports lateral clustering, adhesive strengthening, and interaction with p120ctn. *J. Cell Biol.* **141**, 779-789.
Yap, A. S., Crampton, M. S. and Hardin, J. (2007). Making and breaking contacts: the cellular biology of cadherin regulation. *Curr. Opin. Cell Biol.* **19**, 508-514.